Submitted to *J. Geophys. Res.*

A study of stratospheric chlorine partitioning based on new satellite measurements and modeling

M. L. Santee,[1] I. A. MacKenzie,[2] G. L. Manney,[1,3] M. P. Chipperfield,[4]
P. F. Bernath,[5,6] K. A. Walker,[5,7] C. D. Boone,[5] L. Froidevaux,[1] N. J. Livesey,[1]
and J. W. Waters[1]

Abstract. Two recent satellite instruments — the Microwave Limb Sounder (MLS) on Aura and the Atmospheric Chemistry Experiment Fourier Transform Spectrometer (ACE-FTS) on SCISAT-1 — provide an unparalleled opportunity to investigate stratospheric chlorine partitioning. We use measurements of ClO, HCl, $ClONO_2$, and other species from MLS and ACE-FTS to study the evolution of reactive and reservoir chlorine throughout the lower stratosphere during two Arctic and two Antarctic winters characterizing both relatively cold and relatively warm and disturbed conditions in each hemisphere. At middle latitudes, and at high latitudes at the beginning of winter, HCl greatly exceeds $ClONO_2$, representing $\sim$0.7–0.8 of estimated total inorganic chlorine. Nearly complete chlorine activation is seen inside the winter polar vortices. In the Antarctic, chlorine deactivation proceeds in a similar manner in both winters, with a rapid rise in HCl accompanying the decrease in ClO. In the Arctic, chlorine recovery follows different paths in the two winters: In 2004/2005, deactivation occurs through initial reformation of $ClONO_2$ followed by slow repartitioning between $ClONO_2$ and HCl, in agreement with the canonical view, whereas in 2005/2006, HCl and $ClONO_2$ rise at comparable rates in some regions. The measurements are compared to customized runs of the updated SLIMCAT three-dimensional chemical transport model. Measured and modeled values typically agree well outside the winter polar regions. In contrast, as a consequence of the equilibrium scheme used to parameterize polar stratospheric clouds, the model overestimates the magnitude, spatial extent, and duration of chlorine activation inside the polar vortices.

1. Introduction

Understanding the latitudinal, seasonal, and interannual variations in reactive and reservoir chlorine species, and their relative partitioning, is essential for predicting future stratospheric ozone recovery. Despite numerous observational and modeling studies over the past two decades, aspects of stratospheric chlorine partitioning at both middle and high latitudes remain uncertain. Most previous studies have been hampered by the lack of concurrent measurements of ClO, the predominant form of reactive chlorine in the stratosphere, and $ClONO_2$ and HCl, the two main chlorine reservoirs.

Chlorine partitioning undergoes strong seasonal variations in the lower stratosphere, as low temperatures in the winter polar vortices promote heterogeneous reactions on the surfaces of polar stratospheric clouds (PSCs) or sulfate aerosols that convert chlorine from reservoir to reac-

[1]Jet Propulsion Laboratory, California Institute of Technology, Pasadena, California, USA.
[2]School of GeoSciences, University of Edinburgh, Edinburgh, UK.
[3]Also at Department of Physics, New Mexico Institute of Mining and Technology, Socorro, New Mexico, USA.
[4]School of the Environment, University of Leeds, Leeds, UK.
[5]Department of Chemistry, University of Waterloo, Waterloo, Ontario, Canada.
[6]Now at Department of Chemistry, University of York, Heslington, York, UK.
[7]Now at Department of Physics, University of Toronto, Toronto, Canada.

tive forms. In the Antarctic, ClO is enhanced in the sunlit portions of the vortex by late May/early June [*Santee et al.*, 2003, and references therein]. Virtually all HCl has been converted to reactive forms by early to mid-September, but it is then rapidly regenerated, recovering to near unperturbed abundances by mid-to-late October [*Toon et al.*, 1989; *Murcray et al.*, 1989; *Liu et al.*, 1992; *Kreher et al.*, 1996; *Santee et al.*, 1996; *Notholt et al.*, 1997a]. Modeling studies [*Prather and Jaffe*, 1990; *Douglass et al.*, 1995; *Grooß et al.*, 1997, 2005; *Mickley et al.*, 1997; *Douglass and Kawa*, 1999; *Michelsen et al.*, 1999] have shown that, in the absence of denitrification (the irreversible removal of total reactive nitrogen from the lower stratosphere through the sedimentation of PSC particles, which limits the availability of NO_2 for producing $ClONO_2$), the relative rates of springtime chlorine reservoir formation are controlled by ozone: Under severely depleted conditions typical of Antarctic spring (O_3 $<\sim$0.5 ppmv), HCl production is highly favored. Some studies, however, have found a mismatch between the decay of reactive chlorine and the production of chlorine reservoirs in the Antarctic lower stratospheric vortex [e.g., *Santee et al.*, 1996; *Chipperfield et al.*, 1996].

The Arctic exhibits a large degree of interannual variability, with ClO significantly enhanced by mid-December in some years but not until January (or not at all) in others [e.g., *Toohey et al.*, 1993; *Santee et al.*, 2003, and references therein]. Measurements from ground-based, balloon, aircraft, and satellite instruments have indicated that, after rising temperatures curtail heterogeneous processing, HCl remains depressed, whereas $ClONO_2$ increases rapidly, so that by spring it is well above initial values and exceeds HCl by as much as a factor of two [*Oelhaf et al.*, 1994; *Adrian et al.*, 1994; *Toon et al.*, 1994; *Roche et al.*, 1994; *Blom et al.*, 1995; *Wehr et al.*, 1995; *Müller et al.*, 1996; *Notholt et al.*, 1997b; *Blumenstock et al.*, 1997; *Payan et al.*, 1998; *Galle et al.*, 1999; *Mellqvist et al.*, 2002]. Modeling studies have shown that, for the ozone and odd nitrogen concentrations typical of the Arctic, the primary chlorine recovery pathway is the reformation of $ClONO_2$, which then remains the dominant chlorine reservoir for more than a month as the equilibrium between $ClONO_2$ and HCl is slowly reestablished [*Prather and Jaffe*, 1990; *Lutman et al.*, 1994; *Müller et al.*, 1994; *Douglass et al.*, 1995; *Douglass and Kawa*, 1999; *Michelsen et al.*, 1999]. Recently, however, in situ measurements obtained during the exceptionally cold 1999/2000 winter have been used to challenge the canonical picture of preferential $ClONO_2$ recovery in the Arctic [*Wilmouth et al.*, 2006]. Although HCl was observed to be low and roughly constant on flights into the vortex in January and March, an inferred low bias in the HCl implied the presence of substantially larger amounts of HCl inside the midwinter vortex than expected. Results from a box model suggested that HCl production accompanies $ClONO_2$ production and may be considerably more important in chlorine recovery in the Arctic than previously believed.

Two recent satellite instruments provide measurements of unprecedented scope for investigating chlorine partitioning. The Atmospheric Chemistry Experiment Fourier Transform Spectrometer (ACE-FTS) on the Canadian SCISAT-1 mission has been providing solar occultation profiles of a large number of species, including HCl and $ClONO_2$, since February 2004 [*Bernath et al.*, 2005]. An advanced successor to the Upper Atmosphere Research Satellite (UARS) Microwave Limb Sounder (MLS) was launched as part of NASA's Aura mission in July 2004. Aura MLS measures several key species, including the first simultaneous daily global profiles of HCl and ClO [*Waters et al.*, 2006]. MLS began routine operations in time to observe the 2004 Antarctic late winter, which, by Antarctic standards, was relatively warm and dynamically disturbed, with less ozone loss than in most other recent years; by contrast, the 2005 ozone hole was typical of the last decade [*World Meteorological Organization*, 2007]. The first two Arctic winters observed by Aura also provide a study in contrasts: The 2004/2005 winter was the coldest on record in the lower stratosphere, with large chemical ozone losses [*Manney et al.*, 2006; *Rex et al.*, 2006; *von Hobe et al.*, 2006; *Jin et al.*, 2006; *Singleton et al.*, 2007; *Feng et al.*, 2007], whereas in 2005/2006 a major warming in late January prematurely terminated processing, inhibiting ozone loss [*World Meteorological Organization*, 2006]. In this paper, theoretical understanding of chlorine partitioning throughout the lower stratosphere is assessed by comparing the measurements to customized runs of the updated SLIMCAT chemical transport model [*Chipperfield*, 2006].

2. Measurement and Model Descriptions

2.1. MLS Measurements

MLS measures millimeter- and submillimeter-wavelength thermal emission from the limb of Earth's atmosphere [*Waters et al.*, 2006]. The Aura MLS fields of view point in the direction of orbital motion and vertically scan the limb in the orbit plane, leading to data coverage from 82°S to 82°N latitude on every orbit. Because the Aura orbit is sunsynchronous, MLS observations at a given latitude on either the ascending or descending side of the orbit have essentially the same local solar time. Vertical profiles are measured every $\sim$165 km along the suborbital track and have $\sim$400 km along-track and $\sim$3–10 km across-track horizontal resolution. Vertical resolution is $\sim$3–4 km in the lower to middle stratosphere, depending on the product [*Froidevaux* *et al.*, 2006; *Livesey et al.*, 2005].

In this study we use ClO, HCl, O_3, H_2O, N_2O, and HNO_3 from the first publicly-released Aura MLS dataset, version 1.5 (v1.5) [*Livesey et al.*, 2006]. Single-profile measurement precisions are estimated to be 0.1–0.2 ppbv, 0.1–0.2 ppbv, 0.2–0.3 ppmv, 0.2–0.3 ppmv, 15–30 ppbv, and $\sim$1 ppbv for ClO, HCl, O_3, H_2O, N_2O, and HNO_3, respectively, for the range of altitudes shown here [*Froidevaux et al.*, 2006; *Livesey et al.*, 2005]. For the latitude-band averages on which most of the conclusions of this study are based, the estimated precisions are $\sim$30–50% smaller than these values. Validation analyses for v1.5 HCl, O_3, H_2O, and N_2O indicate overall good agreement (typically within 5–20%) with data from balloon-borne and other space-based instruments [*Froidevaux et al.*, 2006]. In contrast, v1.5 HNO_3 data are biased high by $\sim$10–40% relative to nearly-coincident satellite and balloon measurements [*Froidevaux et al.*, 2006; *Barret et al.*, 2006]. To correct for this artifact, which has been traced to a typographical error in one of the spectroscopy files used in v1.5 processing [*Santee et al.*, 2007b], MLS HNO_3 values have been scaled by 0.7 here. V1.5 ClO measurements compare well with those from the Submillimetre Radiometer (SMR) on the Odin satellite except at retrieval levels below 22 hPa, where they have a systematic negative bias of nearly 0.3 ppbv [*Livesey et al.*, 2005; *Barret et al.*, 2006]. As discussed by *Santee et al.* [2007a], who quantify a similar (but slightly larger) negative bias in the v2.2 MLS ClO data, it is necessary to correct individual ClO measurements by subtracting the estimated negative bias at each of the affected retrieval levels before interpolation to potential temperature surfaces. The estimated magnitudes of the bias in the v1.5 ClO measurements are -0.04, -0.12, -0.24, and -0.29 ppbv at 32, 46, 68, and 100 hPa, respectively.

2.2. ACE-FTS Measurements

ACE-FTS, the primary instrument on SCISAT-1, is a high-resolution (0.02 cm^{-1}) infrared Fourier transform spectrometer that measures solar occultation spectra between 2.2 and 13.3 μm (750–4400 cm^{-1}) [*Bernath et al.*, 2005]. Vertical profiles are retrieved for up to 15 sunrises and 15 sunsets per day, whose latitudes vary over an annual cycle from 85°S to 85°N with an emphasis on the polar regions during winter and spring. Vertical and horizontal resolution of the ACE-FTS measurements are 3–4 km and $\sim$500 km, respectively.

We use ACE-FTS version 2.2 (v2.2) HCl, $ClONO_2$, O_3, HNO_3, N_2O, CH_4, and H_2O data [*Boone et al.*, 2005]. *Froidevaux et al.* [2007] showed that ACE-FTS v2.2 HCl agrees with Aura MLS v2.2 HCl to within $\sim$5%; previously, *Froidevaux et al.* [2006] found similar agreement between v1.5 MLS and v2.1 ACE-FTS HCl. *Dufour et al.* [2006] estimated the total error in v2.2 $ClONO_2$ to be 10–12% in the lower stratosphere, and good agreement (mean differences less than 0.03 ppbv below 26 km) has been demonstrated with MIPAS $ClONO_2$ [*Höpfner et al.*, 2007]. For O_3, we use the v2.2 "ozone update" retrievals, which agree with a number of other satellite datasets to within 5–10%. Dedicated validation papers for ACE-FTS v2.2 measurements are in preparation (for a list see https://brutus.uwaterloo.ca/acedocs/tiki-index.php?page=ACPSpecialIssue). ClO is also retrieved from ACE-FTS spectra, but at this time it remains a research product requiring special handling [K. Walker, personal communication, 2005; *Dufour et al.*, 2006] and is not included in this study.

2.3. Model Calculations

SLIMCAT is a three-dimensional (3D) off-line chemical transport model [*Chipperfield et al.*, 1996; *Chipperfield*, 1999] that has been used extensively to investigate a wide range of polar processes. The model configuration has recently undergone substantial revision [*Chipperfield*, 2006], greatly improving its ability to reproduce polar chemical and dynamical processes [*Chipperfield*, 2006; *Chipperfield et al.*, 2005; *Feng et al.*, 2005]. The updated model has now been used to estimate chemical ozone loss during several Arctic winters [e.g., *Feng et al.*, 2005, 2007; *Goutail et al.*, 2005; *Singleton et al.*, 2005, 2007].

SLIMCAT includes a detailed description of stratospheric chemistry. Photochemical data are taken from JPL 2003 [*Sander et al.*, 2003], except for the Cl_2O_2 photolysis rate, for which the values of *Burkholder et al.* [1990] are used, with a long-wavelength extrapolation to 450 nm [*Stimpfle et al.*, 2004]. The model is forced using specified bottom boundary conditions for surface volume mixing ratios of source gases, taken from *World Meteorological Organization* [2003] scenarios with the addition of 100 pptv of inorganic chlorine, Cl_y, and 6 pptv of inorganic bromine, Br_y, to account for contributions from short-lived species.

The model also includes heterogeneous reactions on cold liquid sulfate aerosols and nitric acid trihydrate (NAT) and ice polar stratospheric clouds (PSCs) [*Chipperfield*, 1999; *Davies et al.*, 2002]. The key reactions are: (1) $ClONO_2 + HCl \longrightarrow Cl_2 + HNO_3$, (2) $ClONO_2 + H_2O \longrightarrow HOCl + HNO_3$, and (3) $HOCl + HCl \longrightarrow Cl_2 + H_2O$. On NAT surfaces the model uses reaction probabilities (γ) of 0.2 for Reaction 1, 0.004 for Reaction 2, and 0.1 for Reaction 3 [*Sander et al.*, 2003]. For cold liquid sulfate aerosols, Reactions 1 and 2 are parameterized following *Hanson and Ravishankara* [1994], with HCl solubility taken from *Luo et al.* [1995]. Reaction 3 is treated as a bulk aqueous reaction with a second order rate constant of 1×10^5 dm^{3}mol^{-1}s^{-1}.

Although a 3D Lagrangian NAT particle sedimentation model has been employed with SLIMCAT to investigate Arctic denitrification [*Mann et al.*, 2002, 2003, 2005; *Davies et al.*, 2005, 2006], none of those studies used coupled chemistry. The "standard" version of SLIMCAT used here and in most other studies of polar processing and ozone loss does not include a microphysical model. Rather, PSCs are assumed to form at the equilibrium NAT saturation temperature, calculated according to *Hanson and Mauersberger* [1988], and to instantaneously grow to a specified size. *Davies et al.* [2006] showed that, compared to microphysical models, NAT equilibrium schemes lead to earlier and more severe denitrification than observed. This overestimation of PSC occurrence and denitrification has ramifications for both the activation and the deactivation of chlorine in the model.

The seasonal simulations analyzed here have $2.8^\circ \times 2.8^\circ$ horizontal resolution and 50 vertical levels from the surface to 3000 K ($\sim$60 km), with purely isentropic surfaces above 350 K and a spacing of $\sim$20 K between 450 and 680 K. For many species SLIMCAT is initialized using output from a lower-resolution ($7.5^\circ \times 7.5^\circ$) multi-annual run [e.g., *Feng et al.*, 2005; *Singleton et al.*, 2005]. For O_3 and H_2O, initial values are taken from MLS measurements. Initial HCl is also taken from MLS, with model initial $ClONO_2$ and reactive chlorine adjusted such that the original model Cl_y is retained (note that no further adjustment of $ClONO_2$ or reactive chlorine is performed as the run progresses). Initial HNO_3 is based on MLS data in the lower stratosphere, scaled by 0.7 to account for the known high bias in v1.5 MLS HNO_3 measurements (see section 2.1); no adjustment to other NO_y species is made, and above 1050 K the initialization reverts to the original model HNO_3 field. Similarly, N_2O initialization is based on MLS measurements below 1450 K, merged with the original model values above that level. For each MLS measurement an equivalent model value, interpolated to the same location, is taken at the nearest available time (always within 15 minutes).

Horizontal winds and temperatures for these simulations are from the European Centre for Medium-Range Weather Forecasts (ECMWF) analyses [*Simmons et al.*, 2005]. For some of the winters examined here, corresponding SLIMCAT runs were performed using U.K. Met Office analyses [*Swinbank et al.*, 2002]. The general characteristics of model/measurement agreement were found to be similar for ECMWF- and Met Office-driven simulations.

Off-line calculations [*MacKenzie et al.*, 1996] are performed to infer total reactive chlorine (ClO_x = ClO + 2 $\times$ Cl_2O_2) from MLS ClO using the same photochemical parameters and photolysis scheme as SLIMCAT. Because Cl_2O_2 is assumed to be in photochemical equilibrium with ClO, the calculations are performed only for daylight (solar zenith angles less than 89°) measurements. The largest uncertainty in inferred ClO_x lies in the Cl_2O_2 photolysis rate. Equilibrium Cl_2O_2 values calculated using the long-wavelength extrapolation of Cl_2O_2 cross sections from *Burkholder et al.* [1990] are 40–50% smaller than those given by JPL 2003 cross sections but are more consistent with Cl_2O_2 measurements [*Stimpfle et al.*, 2004].

3. Northern Hemisphere Seasonal Evolution

3.1. The 2004/2005 Arctic Winter

The Northern Hemisphere lower stratosphere was extremely cold throughout most of the 2004/2005 winter. Temperatures were low enough for PSCs on 95 days, more than any other Arctic winter on record, and low temperatures also covered a much broader area than usual [*Kleinböhl et al.*, 2005; *Manney et al.*, 2006]. In addition, the 2004/2005 lower stratospheric polar vortex was stronger than average, but it was also very active and distorted, with frequent intrusions of extravortex air and mixing between vortex edge and core regions, particularly during late winter [*Manney et al.*, 2006; *Schoeberl et al.*, 2006].

The evolution of chlorine partitioning in the 2004/2005 winter is shown in Figure 1. Measured and modeled quantities are broadly consistent, but MLS indicates significant vortex-averaged chlorine activation from the beginning of January, whereas SLIMCAT indicates the onset of enhanced ClO and an abrupt decline in HCl (compare the slopes of the HCl contours) more than a month earlier. The poor coverage of ACE-FTS inside the polar vortex in December (see https://database.uwaterloo.ca/validation/measurementdescription.php for ACE-FTS occultation locations) precludes comparison of measured and modeled $ClONO_2$ in early winter, but data from the beginning of January suggest model overestimation of $ClONO_2$ depletion. Furthermore, reactive chlorine extends over a larger vertical domain and maximum abundances persist longer at the end of winter in the model than in the MLS data.

The MLS data in Figure 1 indicate maximum ClO enhancement near 490 K ($\sim$20 km) for much of the winter, so we focus on that level in Figure 2, which shows daily averages similar to zonal means but calculated as a function of equivalent latitude (EqL, the latitude encircling the same area as a given contour of PV [*Butchart and Remsberg*, 1986]) to provide a vortex-centered view. Again, both ClO and HCl show earlier and more substantial chemical processing in the model than observed by MLS; modeled chlorine activation also extends to slightly lower EqLs. Similar results are obtained throughout the lower stratosphere (not shown), with the degree of model over-activation even more striking at higher altitudes.

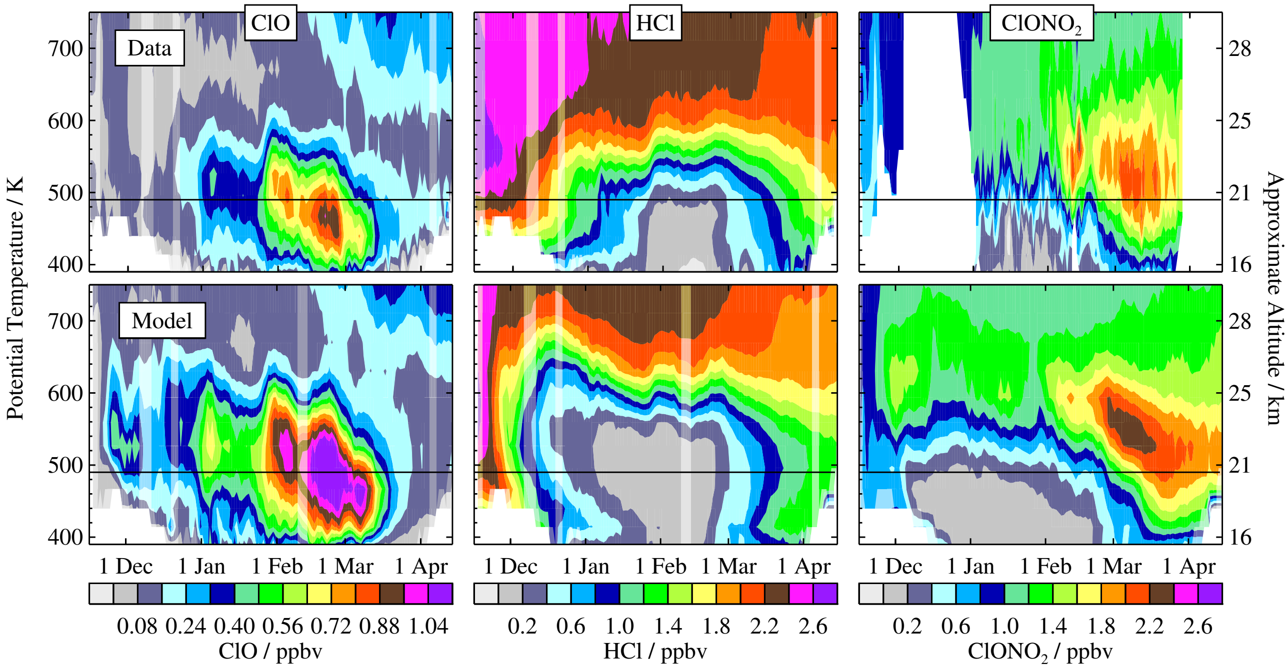

Figure 1. Time series over the 2004/2005 Arctic winter of vortex-averaged quantities calculated within the 1.6×10^{-4} s^{-1} contour of scaled potential vorticity (where sPV, which has roughly the same values on isentropic surfaces throughout the stratosphere, is calculated using the method of *Manney et al.* [1994]) as a function of potential temperature. (Top row) ClO and HCl data from Aura MLS and $ClONO_2$ data from ACE-FTS. Only daytime (ascending) data are shown for ClO; the individual measurements contributing to the daily averages have been adjusted to correct for a known negative bias in the MLS ClO data as discussed in section 2.1. Small gaps in the data have been filled by running the daily averages through a Kalman smoother (as described by *Santee et al.* [2004]); paler colors denote the regions in which the estimated precision of the interpolated values is poor (i.e., MLS data are not available). ACE-FTS $ClONO_2$ data have also been smoothed slightly to enhance the legibility of the plots, but the large gaps arising from the sparse sampling of the ACE-FTS measurements within the polar vortex at the beginning and end of the observation period have not been filled. The black horizontal line in each panel marks the 490 K level. (Bottom row) Corresponding SLIMCAT model results, sampled at the MLS measurement locations and times. For consistency, both measurements and model results have been interpolated to potential temperature surfaces using NASA's Global Modeling and Assimilation Office Goddard Earth Observing System Version 4.0.3 (GEOS-4) temperatures [*Bloom et al.*, 2005].

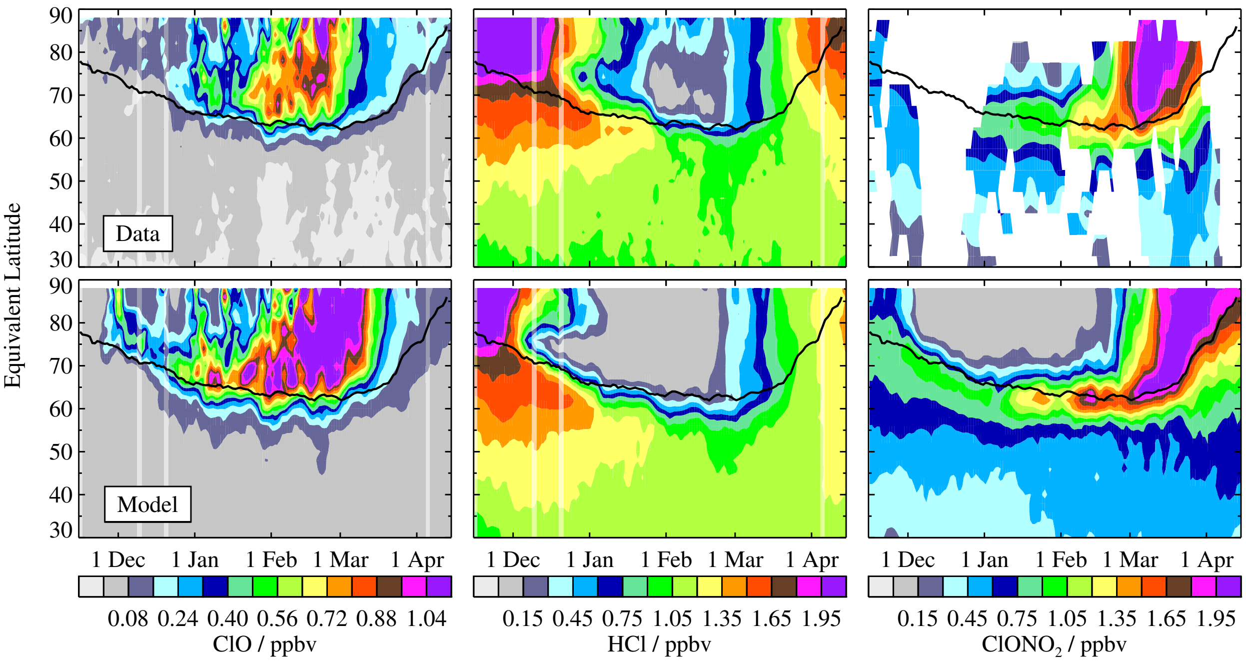

Figure 2. Time series over the 2004/2005 Arctic winter as a function of equivalent latitude (EqL) at 490 K. (Top row) ClO and HCl data from MLS and $ClONO_2$ data from ACE-FTS. Only daytime (ascending) data are shown for ClO; the individual measurements contributing to the daily averages have been adjusted to correct for a known negative bias in the MLS ClO data as discussed in section 2.1. Small gaps in the data have been filled using a Kalman smoother as in Figure 1. The $1.6\times10^{-4}\,s^{-1}$ contour of sPV is overlaid in black to demark the approximate edge of the polar vortex. (Bottom row) Corresponding SLIMCAT model results, sampled at the MLS measurement locations and times.

A quantitative examination is shown in Figure 3, where daily averages of MLS and ACE-FTS data are compared with SLIMCAT results in 5° EqL bands from 60° to 80° EqL to distinguish variations in behavior between vortex interior and edge regions. ClO_x inferred from MLS ClO (section 2.3) is also compared to the model, along with estimates of Cl_y (the sum of reactive chlorine and the two reservoirs). Similarly, Figure 4 shows the evolution of the fraction of total inorganic chlorine residing in the different species. Variations in the geographic sampling of inherently inhomogeneous fields can give rise to significant day-to-day scatter in these plots. To minimize the possibility of sampling biases affecting the comparisons, equivalent points are included in the averages of all MLS species (i.e., only data passing the quality control criteria for all species and for which the solar zenith angle is less than 89°), and corresponding profiles are selected for MLS and SLIMCAT averages. Unfortunately, the sampling pattern of ACE-FTS is distinctly different from that of MLS, so the ACE-FTS averages do not encompass the same air masses. The excellent agreement between ACE-FTS and MLS HCl (cf. solid green circles and triangles) throughout the winter lends confidence in the representativeness of the ACE-FTS averages, although, as seen below, in some cases the ACE-FTS sampling leads to ambiguity in interpreting these time series.

EqL-band averages like those in Figures 3 and 4 for northern midlatitudes (not shown) indicate that HCl greatly exceeds $ClONO_2$ throughout the study period, representing ∼0.7–0.8 of Cl_y compared to ∼0.2–0.3 for $ClONO_2$. The high-EqL measurements paint a similar picture for early winter, before significant processing has occurred. On the basis of ACE-FTS observations, *Dufour et al.* [2006] reported that HCl began to decline in early January, with ClO significantly enhanced only after 10 January. MLS data show, however, that changes in chlorine partitioning at the highest EqLs occur in early-to-middle December, whereas they are not evident in the 60–65° EqL band until January (Figure 3). Because ACE-FTS samples outside or near the edge of the vortex in December, it does not capture the onset of processing.

As noted above, SLIMCAT overestimates chlorine activation, with modeled HCl smaller and ClO_x larger than measured by late November in the vortex core and by early January near the vortex edge. Although the model initially agrees fairly well with ACE-FTS $ClONO_2$, by January it underestimates $ClONO_2$ at the highest EqLs. It is unlikely that the greater degree of chemical processing in the model indicated in Figures 1–4 can be attributed to a

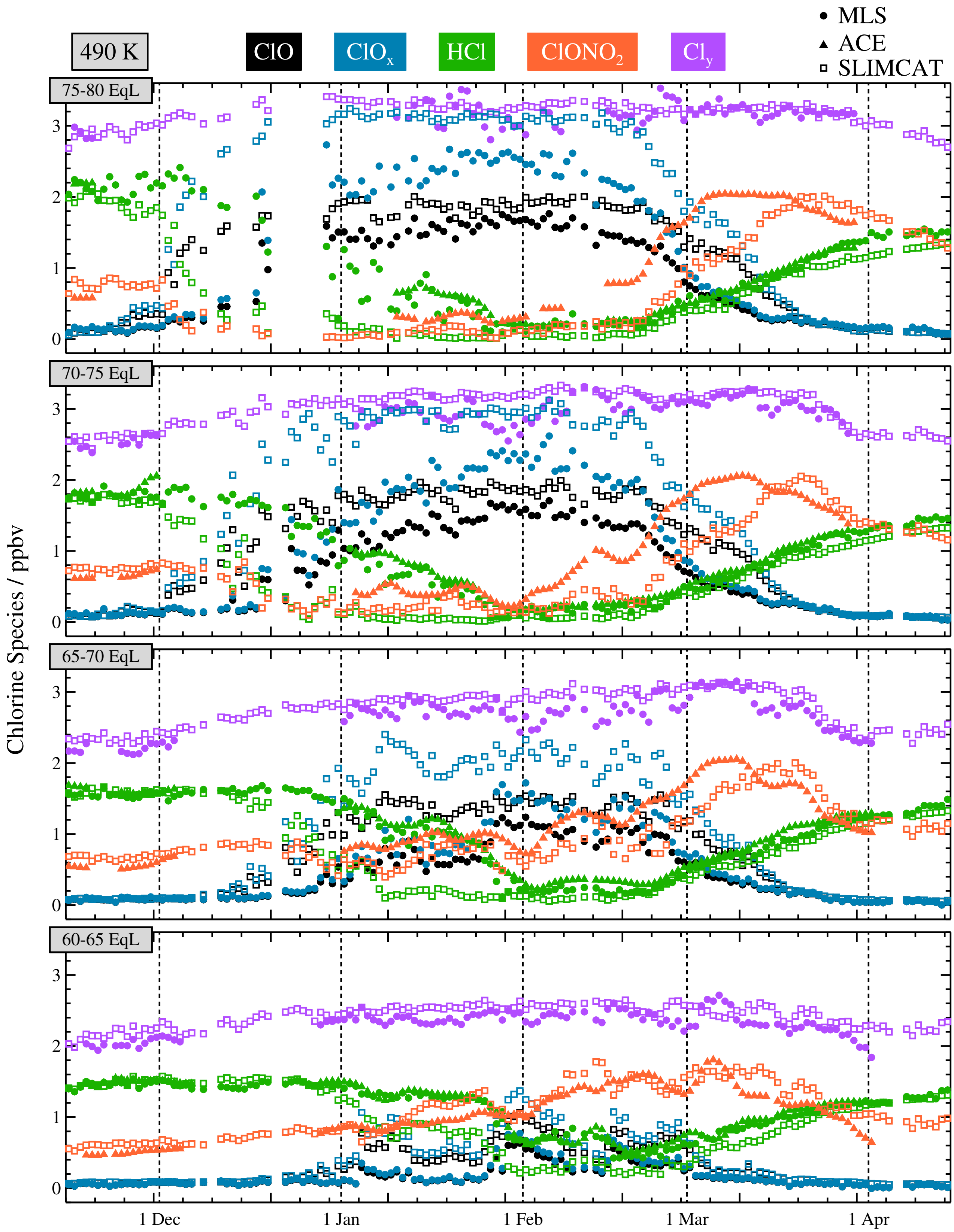

Figure 3. Time series over the 2004/2005 Arctic winter of chlorine species at 490 K. Daily means have been calculated by binning the data into 5° EqL bands and averaging. For MLS ClO, adjustments are made for the known negative bias as discussed in section 2.1. Dashed vertical lines demark calendar months. Solid symbols denote measurements (circles=MLS, triangles=ACE-FTS); open squares denote SLIMCAT model results. Different colors represent different species as indicated in the legend. ClO_x=ClO+2×Cl_2O_2, calculated from the MLS ClO data as described in section 2.3; Cl_y=ClO_x+HCl+$ClONO_2$, using MLS HCl and ACE-FTS $ClONO_2$ measurements. For consistency, model ClO_x and Cl_y are defined similarly.

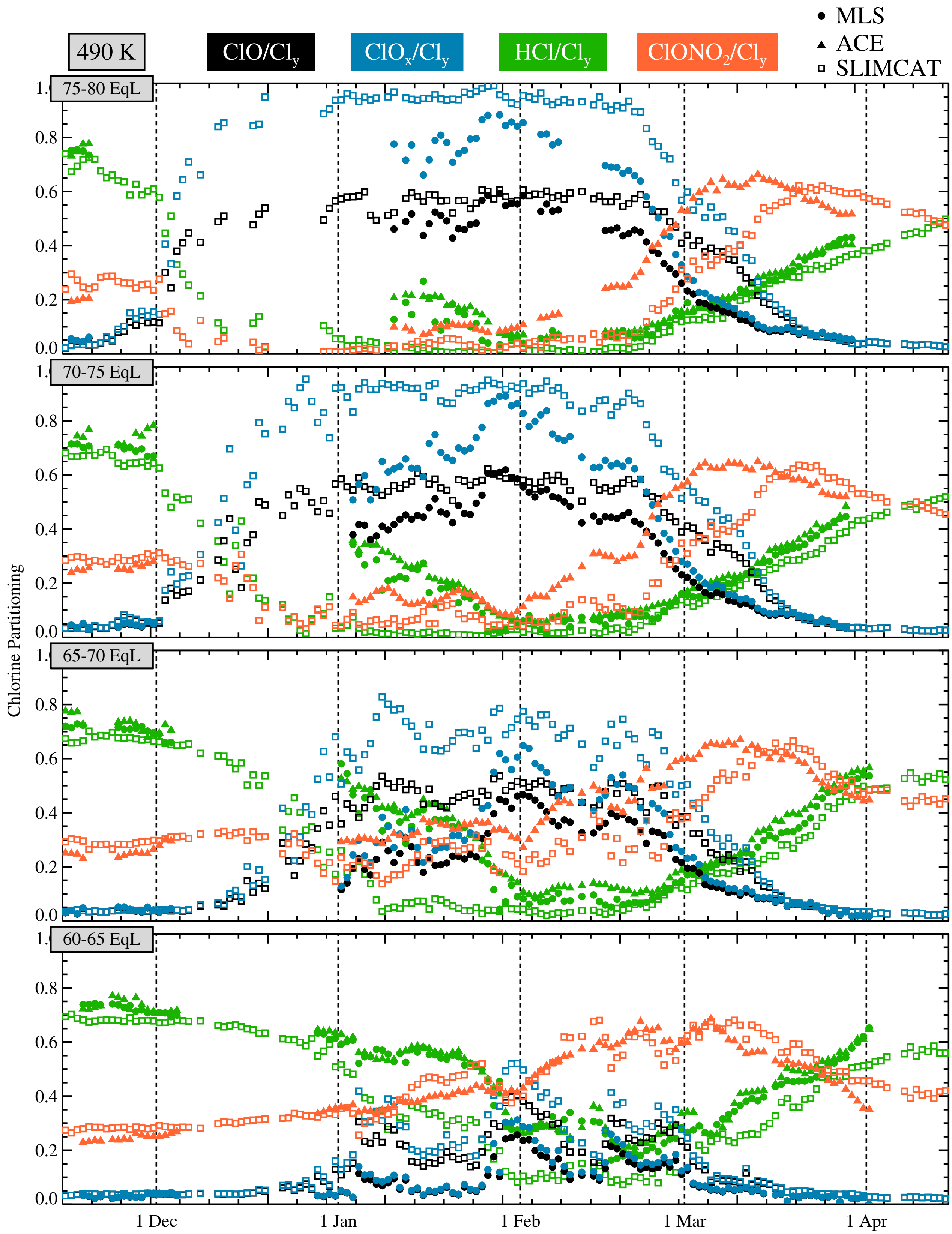

Figure 4. As in Figure 3, for the fraction of total inorganic chlorine (Cl_y) residing in ClO, ClO_x, HCl, and $ClONO_2$ at 490 K. Note that fewer measurement points appear here for some of the species than in Figure 3 because data from both ACE-FTS and MLS are needed to define Cl_y.

systematic low bias in the forcing ECMWF temperatures. Zonal mean temperature differences for December-January-February 2004/2005 between ECMWF and CHAllenging Minisatellite Payload (CHAMP) temperatures are less than 0.5 K in the northern polar lower stratosphere [A. Gobiet, personal communication, 2006], comparable to the biases seen in similar comparisons for previous years [*Gobiet et al.*, 2005]. Biases of this magnitude are not sufficient to account for SLIMCAT's overly enthusiastic chlorine activation.

We also investigated whether errors in modeled transport influenced chemical processing by producing unrealistic trace gas distributions. Comparisons with measurements of N_2O (Figure 5) and CH_4 (from ACE-FTS, not shown) indicate that the revised SLIMCAT model generally reproduces the diabatic descent, as found by *Feng et al.* [2005], especially during the first half of the study period. Agreement is not perfect; either the modeled descent is slightly too strong (as found also by *Feng et al.* [2007]), or the model does not have quite enough mixing into the vortex to dilute the signature of descent, especially at lower levels. Again, however, the differences are insufficient to explain the discrepancy in reactive chlorine.

The earlier and more extensive activation of chlorine in the model appears to arise from the NAT equilibrium scheme used to parameterize PSCs. Maps of SLIMCAT results (not shown) indicate localized HNO_3 depletion as soon as temperatures dip below the NAT threshold, as early as 20 November to 1 December depending on the altitude, with immediate HCl depletion and ClO enhancement in and just downstream from the PSC region. In contrast, localized depletion in HNO_3 and HCl and significant enhancement in ClO are not seen in MLS data until $\sim$10 December. These small pockets of processed air are smeared out in the averages shown in previous plots, which consequently suggest an even greater lag between the onset of modeled and measured processing. The dramatic difference in the evolution of MLS and SLIMCAT HNO_3 is illustrated in Figure 5, which shows that modeled HNO_3 is almost completely depleted by early January at the highest EqLs below $\sim$500 K. Initializing the model with MLS H_2O may have exacerbated this problem, since that tended to increase H_2O abundances over those in the original initialization field and thus increased the temperature at which NAT formation occurs. Overestimation of chlorine activation appears to be largely independent of initial conditions, however, as *Feng et al.* [2005] also reported pronounced enhancement in model reactive chlorine by 1 December (the first date shown) in several Arctic winters. These results underscore the difficulty in realistically simulating chlorine activation, a rapid process triggered by crossing a narrow threshold of physical conditions.

Figures 3 and 4 show that observed HCl continues to exceed $ClONO_2$ until late January, at which time each reservoir represents only $\sim$0.1 of Cl_y in the vortex core. ClO_x/Cl_y peaks at $\sim$0.8–0.9 in late January/early February, attaining larger values at higher EqLs as seen in UARS MLS ClO [*Santee et al.*, 2003]. The approximation to Cl_y based on MLS and ACE-FTS measurements departs significantly from initial values in the vortex core during the period of peak activation. This is in contrast to modeled Cl_y, which stays relatively flat (in terms of day-to-day variations; the slight growth in model Cl_y over the course of the winter results from descent bringing down air in which more of the source gases have photolyzed, releasing chlorine). That measured Cl_y varies by as much as 0.5 ppbv only at the highest EqLs and only during late January and February may suggest a contribution from an unmeasured species in polar night. *Wilmouth et al.* [2006] attributed a $\sim$0.5–1.0 ppbv discrepancy in the chlorine budget in midwinter 1999/2000 to the presence of significant concentrations of Cl_2 in darkness. HOCl may also play a minor role, and other unmeasured forms of inorganic chlorine have been proposed [e.g., *Sander et al.*, 1989]. On the other hand, the observed variability may simply be related to the sampling of the ACE-FTS measurements relative to the shape of the vortex, as discussed further below and explored in detail by *Manney et al.* [2007].

Both ACE-FTS and MLS provide unambiguous evidence that HCl abundances deep inside the midwinter vortex remain relatively constant at $\sim$0.1–0.2 ppbv for several weeks, during which MLS observes ClO to decrease and ACE-FTS observes $ClONO_2$ to increase. It is possible that the steep slope in $ClONO_2$ in early and mid-February is not a real atmospheric signal but merely an artifact. The sparse ACE-FTS sampling combined with strong PV and trace gas gradients across the vortex edge could induce large variations in averages calculated within 5°-wide EqL bins, especially since from early February onward the vortex was very dynamically active, with episodes of strong wave activity and mixing until the final warming in mid-March [*Manney et al.*, 2006]. On the other hand, the undulations seen in ACE-FTS $ClONO_2$ later in February and March and the sharp drop at lower EqLs in late March are strongly correlated with changes in N_2O and CH_4 (not shown), indicating a dynamical and/or sampling origin, whereas the tracers show no major variations in early February. This strongly suggests that the observed increases in $ClONO_2$ in early February are chemical in nature. Thus substantial recovery of $ClONO_2$ precedes that of HCl at the end of the 2004/2005 winter.

$ClONO_2$ peaks in early-to-middle March, at values much higher than observed at the beginning of winter ($\sim$2 ppbv; $ClONO_2/Cl_y$ $\sim$0.6–0.7, Figure 4), and then slowly declines as chlorine is shifted into HCl, the longer-lived reservoir.

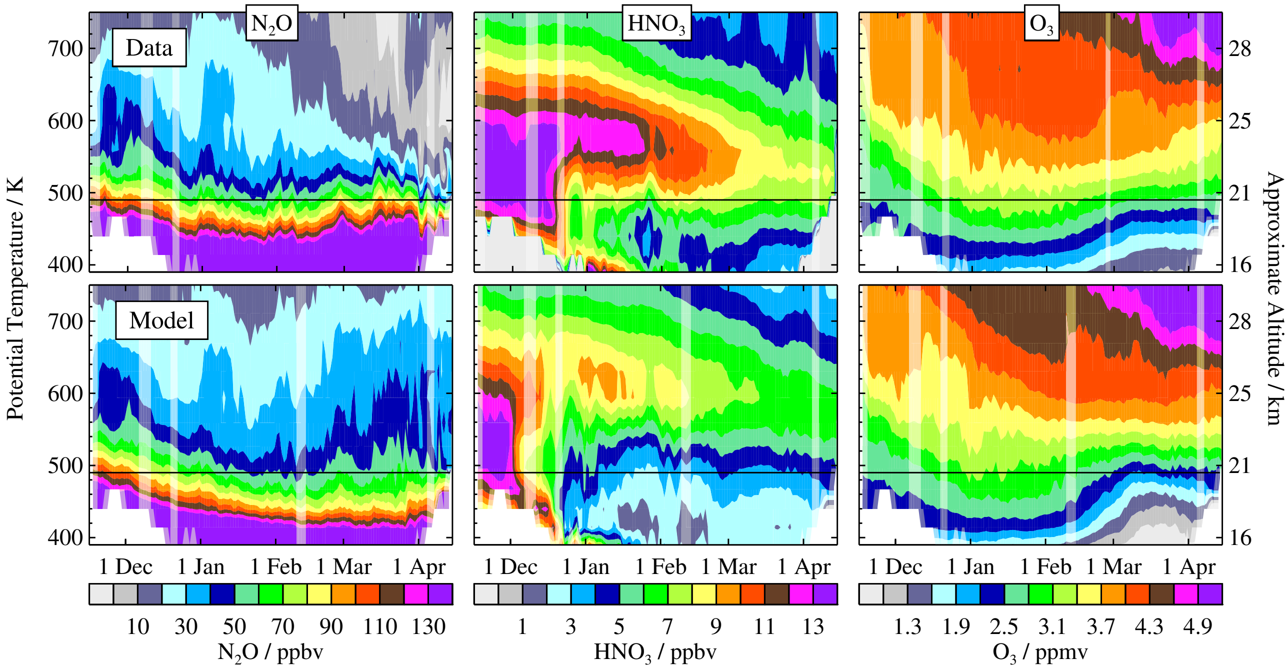

Figure 5. As in Figure 1, for MLS N_2O, HNO_3, and O_3 and corresponding SLIMCAT model results. MLS HNO_3 values have been scaled by 0.7 to account for a known high bias in v1.5 HNO_3 data (see section 2.1).

Although starting to level off, HCl has not quite recovered to pre-winter abundances by the end of the study period, when HCl and $ClONO_2$ fractions are roughly equal at ∼0.4–0.6, depending on the EqL band. Thus ACE-FTS and MLS measurements during the 2004/2005 winter clearly support the canonical view of chlorine deactivation in the Arctic (section 1), with the primary pathway the reformation of $ClONO_2$, followed by slow repartitioning between $ClONO_2$ and HCl. This is in contrast to the findings of *Wilmouth et al.* [2006], who conclude that HCl production approached that of $ClONO_2$ during the initial recovery phase in 1999/2000. We do agree, however, that some HCl remains in the vortex even when chlorine is at peak activation; the lowest midwinter HCl mixing ratios measured by ACE-FTS and MLS (Figure 3) are consistent with the minimum HCl value inferred by *Wilmouth et al.* [2006].

Wilmouth et al. [2006] point out that their results pertain to the portions of the Arctic vortex sampled by the ER-2 during the exceptionally cold 1999/2000 winter and may represent an atypical situation. The 2004/2005 winter studied here, however, was also exceptionally cold (in fact, by many measures it was even colder, if considerably less quiescent dynamically). Thus relative rates of recovery in HCl and $ClONO_2$ like those reported by *Wilmouth et al.* [2006] might have been expected in 2004/2005.

The model simulations in Figure 3 do not mirror observed $ClONO_2$. One possible cause for the discrepancy is that, because the model results are sampled at MLS measurement locations and times, they are not well-aligned with the local solar times of the ACE-FTS occultations, which correspond to sunrise measurements before mid-February and sunset measurements after that time. Comparisons between averages of daytime-only and nighttime-only SLIMCAT values (not shown) suggest, however, that the small changes in $ClONO_2$ over the diurnal cycle cannot account for the model/measurement divergence seen in Figure 3.

Previous studies have shown that chlorine partitioning is highly sensitive to ozone abundances, with lower ozone mixing ratios in late winter leading to preferential reformation of HCl [e.g., *Douglass et al.*, 1995; *Grooß et al.*, 1997; *Mickley et al.*, 1997; *Douglass and Kawa*, 1999; *Grooß et al.*, 2005]. In order to successfully simulate the relative abundances of the reservoir species it is necessary that measured and modeled ozone agree. Figure 5 shows that as the cumulative ozone loss resulting from the greater model chlorine activation outpaces the larger influx of ozone into the lower stratosphere from the stronger model descent, measured and modeled ozone values diverge at the highest EqLs. Unlike earlier versions of SLIMCAT, which underestimated Arctic ozone loss, the version used here slightly overestimates the loss observed in 2004/2005 [*Feng et al.*, 2007; *Singleton et al.*, 2007]. The discrepancy between measured and modeled ozone is not yet that substantial by early-to-middle February, however, and is also smaller at 490 K than at lower altitudes. Furthermore, the model does not exhibit a rapid rise in HCl to compensate for the slow response in $ClONO_2$; modeled and measured values of HCl agree well during this period. The model simply fails to form $ClONO_2$ as rapidly as observed.

The underestimation of $ClONO_2$ during the initial recovery period most likely arises because SLIMCAT's ability to form $ClONO_2$ is limited by the availability of NO_2, which is produced through HNO_3 photolysis and reaction with OH. Because the model overestimates the prevalence of PSCs and/or the degree of denitrification, gas-phase HNO_3 is suppressed, allowing ClO to remain enhanced. The modeled deactivation process is thus fundamentally similar to that indicated by the measurements, but the longevity of modeled PSC activity induces a shift of several weeks in its timing. SLIMCAT $ClONO_2$ peaks in mid-to-late March, whereas the measurements indicate that it is already starting to decline by that time as chlorine is converted into HCl. The model therefore slightly overestimates $ClONO_2$ and underestimates HCl toward the end of the study period in most EqL bins.

Corresponding plots for other potential temperature surfaces (not shown) reveal a similar picture of vortex chlorine activation and deactivation, although small differences in the timing of these processes are evident. As can be seen in Figure 1, chlorine is activated at roughly the same time throughout the lower stratosphere, but ClO remains enhanced about a month longer at 460 K than at 580 K. A similar downward progression in the altitude of peak ClO has also been reported in UARS MLS [*Santee et al.*, 2003] and Antarctic ground-based [*de Zafra et al.*, 1995; *Solomon et al.*, 2002] measurements, consistent with the effects of diabatic descent and the patterns in temperatures and PSC formation in late winter. In addition, at higher altitudes HNO_3 abundances are larger (Figure 5), and *Chipperfield et al.* [1997] have shown that the rate of release of NO_2 from HNO_3 is about a factor of two faster, leading to earlier recovery.

3.2. The 2005/2006 Arctic Winter

The 2005/2006 Arctic winter started out with an unusually strong cold vortex, but a major stratospheric sudden warming in mid-January effectively terminated winter conditions, curtailing chemical processing [*World Meteorological Organization*, 2006]. Prior to the warming, the vortex was highly elongated, with the cold pool situated well off the pole in the region of both sunlight and strong winds. These conditions promoted significant chlorine activation several weeks earlier than in 2004/2005 (cf. Figures 1 and 6). ClO also peaked at higher altitude, near 520 K. SLIMCAT again calculates chlorine activation that is considerably greater in magnitude, spatial extent, and duration than observed (Figures 6 and 7). As for the previous winter, comparisons of measured and modeled HNO_3 (Figure 8) indicate that the exaggerated activation in the model can be attributed to overly abundant PSCs.

In addition to earlier onset of substantial activation, the evolution of chlorine partitioning differs from that in the previous year in several other ways (cf. Figures 3 and 7). In 2004/2005, chlorine is initially deactivated into $ClONO_2$, with $ClONO_2$ abundances exceeding those of HCl for 1–2 months. In 2005/2006, HCl rises at roughly the same rate as $ClONO_2$ between 65° and 75° EqL (Cl_y fraction of both $\sim$0.4–0.5 at the beginning of February, not shown). At 75–80° EqL, however, $ClONO_2$ reforms first and briefly surpasses HCl at the end of January/beginning of February. Thus, unlike in 2004/2005, a different picture of chlorine deactivation is seen at different locations in the vortex: in accord with the canonical view in the innermost core, but in accord with that presented by *Wilmouth et al.* [2006] elsewhere. Even at 75–80° EqL, $ClONO_2$ plays a less important role than in the previous winter, with $ClONO_2/Cl_y$ never quite reaching 0.6 and with the period of $ClONO_2$ in excess of HCl lasting only a few weeks. Furthermore, the relative abundances of the two reservoirs vary with altitude; whereas in 2004/2005 the characteristics of chlorine deactivation are essentially similar at all potential temperature levels, in 2005/2006 the recovery rates for HCl and $ClONO_2$ at 70–75° EqL are roughly comparable at the top three levels but $ClONO_2$ reformation is faster at 490 and 460 K (Figure 9). As at 520 K, however, latitudinal differences are seen at these levels.

The patterns of chlorine partitioning in Figures 7 and 9 may have been influenced by mixing. Even before the major warming, the 2005/2006 winter was more dynamically active than the previous year, with potentially large exchange between extravortex, edge, and vortex interior air. ACE-FTS sampling may also be a factor. As discussed earlier, EqL band averages based on only a few measurements near the edge of the collar region may exhibit day-to-day variations unrelated to chemical changes. ACE-FTS tracer measurements, however, do not reflect substantial heterogeneity in the sampled air masses until late January (Figure 8), well after the start of the rapid increase in HCl. Moreover, MLS indicates HCl production rates very similar to those from ACE-FTS at all EqLs and altitudes. Thus, even without considering $ClONO_2$, clear differences in chlorine reservoir reformation are evident in the two winters.

Differences are also observed in other species; in particular, although ozone abundances are initially very similar to those at the beginning of the 2004/2005 winter, by

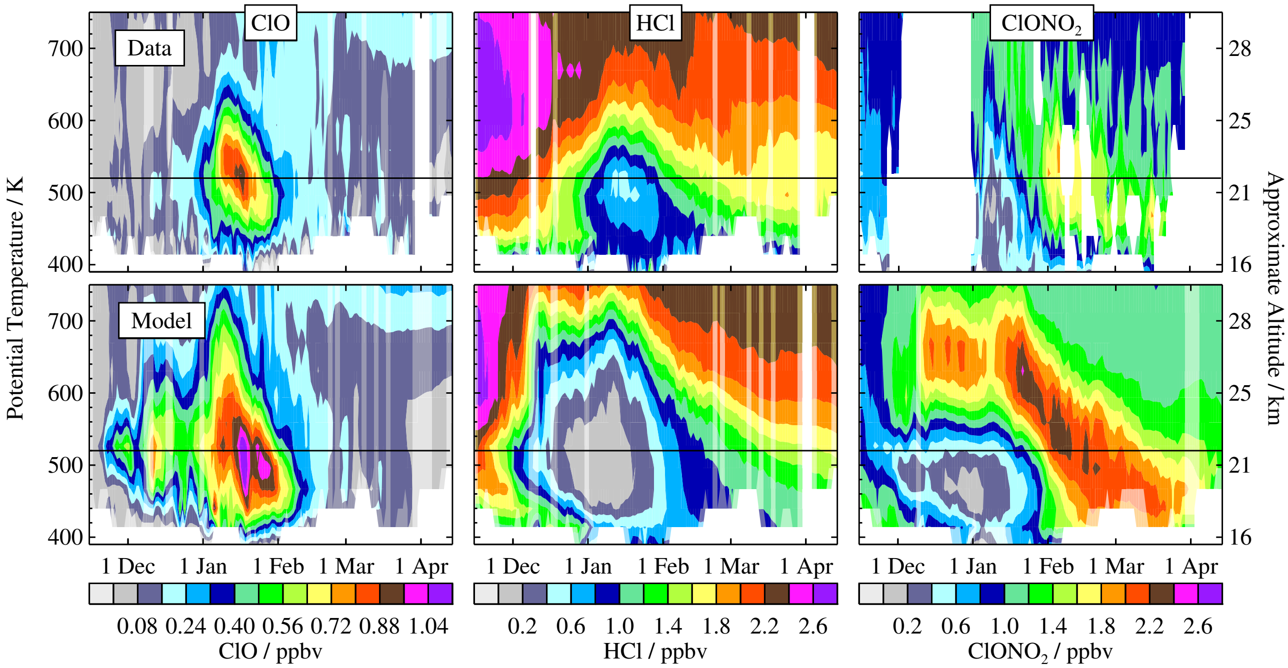

Figure 6. As in Figure 1, for the 2005/2006 Arctic winter. The black horizontal line in each panel marks the 520 K level.

January they are significantly smaller in much of the vortex. Since ClO is already highly enhanced, chemical ozone loss may be partially responsible for the lower ozone mixing ratios in January 2006 [*World Meteorological Organization*, 2006]. In addition, the fact that N_2O mixing ratios are higher (not shown) suggests that diabatic descent is weaker in 2005/2006 than in 2004/2005, contributing to lower ozone values. The inference of weaker descent in 2005/2006 is consistent with differences in the GEOS-4 diabatic heating rates between the two winters.

Detailed examination (not shown) reveals that where January 2006 ozone abundances are similar to those in 2005 (e.g., at 75–80° EqL at 520 K or 70–80° EqL at 490 K), $ClONO_2$ recovery precedes that of HCl, whereas where they are ∼0.5 ppmv less than those in 2005 (e.g., at 65–70° EqL at 520 and 490 K), $ClONO_2$ and HCl recovery rates are comparable. This appears to be consistent with the results of *Douglass and Kawa* [1999], who showed that, in comparison to 1992, a colder and more persistent vortex delayed deactivation and exacerbated ozone loss in 1997, when HCl recovered much more rapidly. Using a 3D chemical transport model, *Douglass and Kawa* [1999] found that in 1997 low temperatures and low ozone combined to push chlorine partitioning toward HCl, with HCl/Cl_y similar to that in the Antarctic (∼0.8–0.9). The difference in ozone between the parcels in 1992 and those in 1997 in which HCl increased was ∼0.5 ppmv; temperature was also found to play a nonnegligible role in promoting HCl production. The meteorological and chemical ozone loss conditions in 2006 are very different from those in 1997 [*Douglass and Kawa*, 1999] or 2000 [*Wilmouth et al.*, 2006], and a dedicated set of model sensitivity tests (beyond the scope of this paper) is needed to confirm the critical role of ozone in controlling chlorine reservoir reformation for the specific conditions of the 2005/2006 winter.

4. Southern Hemisphere Seasonal Evolution

4.1. The 2005 Antarctic Winter

The lower stratosphere was colder than average during much of the 2005 Antarctic winter, with temperatures low enough to support PSCs over a substantial portion of the vortex from late May until mid-to-late September [*World Meteorological Organization*, 2005]. The vortex was also very strong, particularly from the beginning of July through October.

An overview of the chlorine partitioning throughout the 2005 Antarctic winter is shown in Figures 10 and 11. ClO starts to increase in the sunlit portions of the vortex by late May (not shown), but significant enhancement is not evident in the vortex averages until early June. Chlorine activation continues to intensify until September, after which deactivation is rapid, with steep slopes in the ClO and HCl contours. Vortex-averaged $ClONO_2$ values are high throughout

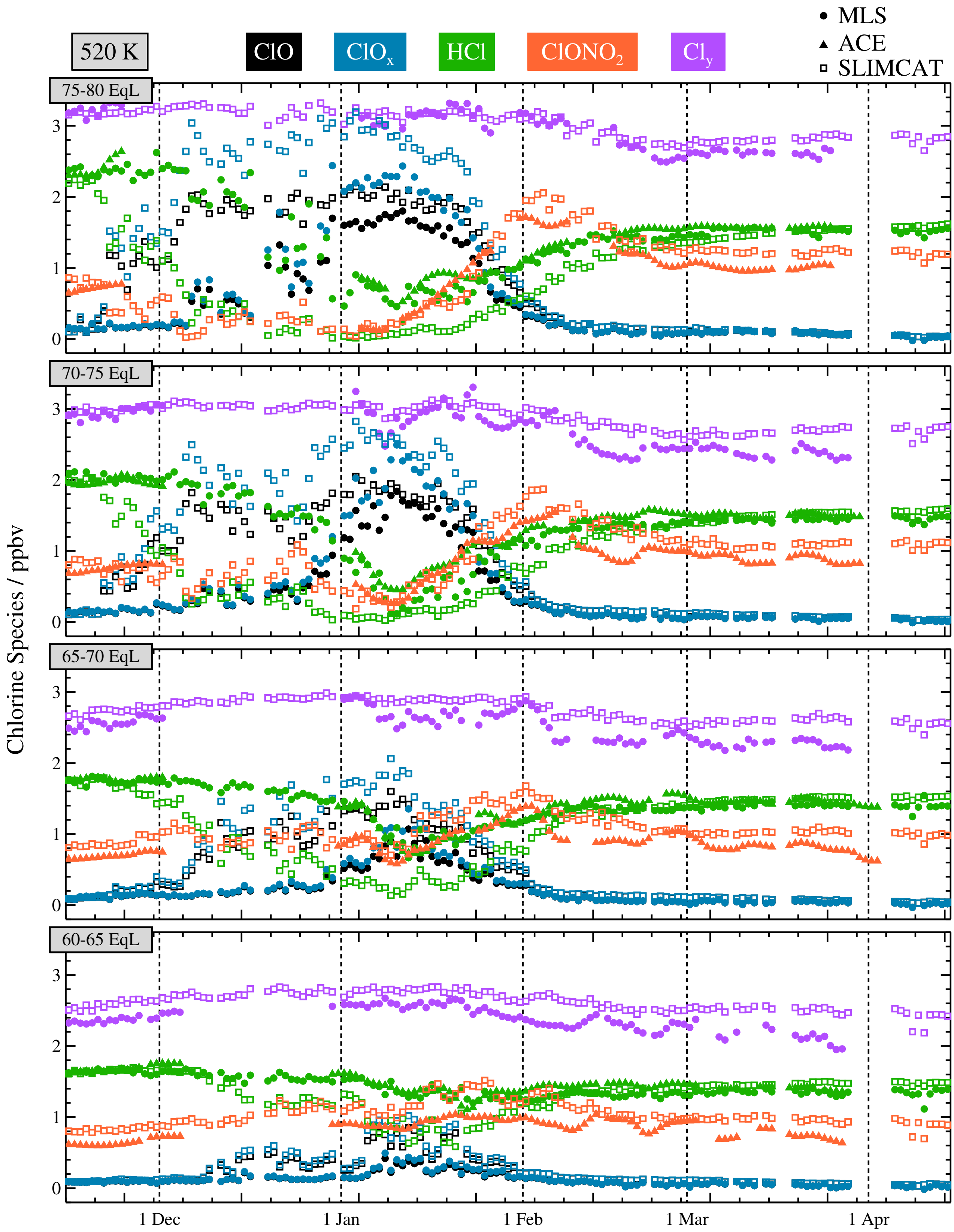

Figure 7. As in Figure 3, for the 2005/2006 Arctic winter at 520 K.

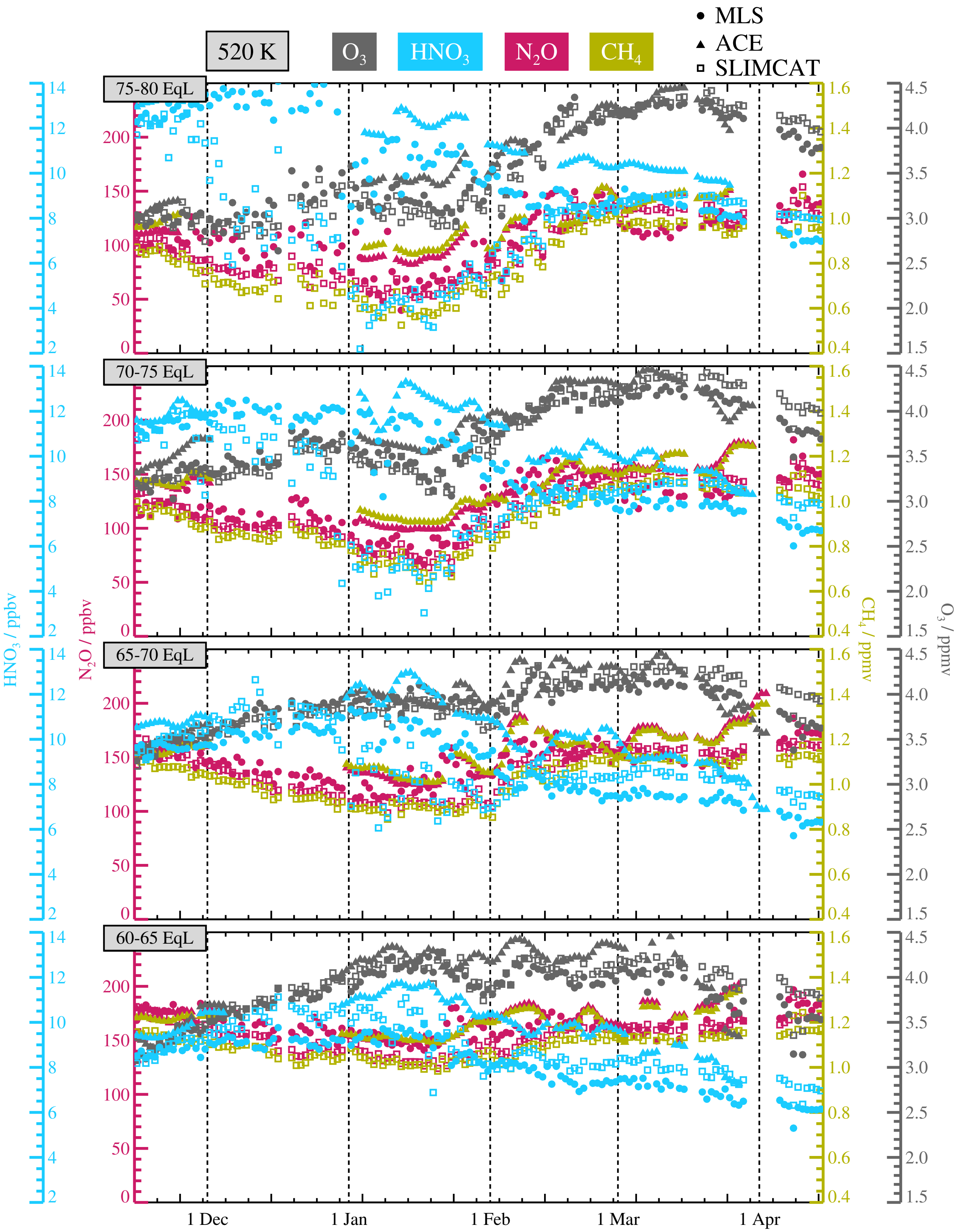

Figure 8. Time series over the 2005/2006 Arctic winter of N_2O, CH_4, HNO_3, and O_3 at 520 K, calculated as in Figure 7. MLS HNO_3 values have been scaled by 0.7 to account for a known high bias in v1.5 HNO_3 data (see section 2.1). Solid symbols denote measurements (circles=MLS, triangles=ACE-FTS); open squares denote SLIMCAT model results. Different colors represent different species as indicated in the legend.

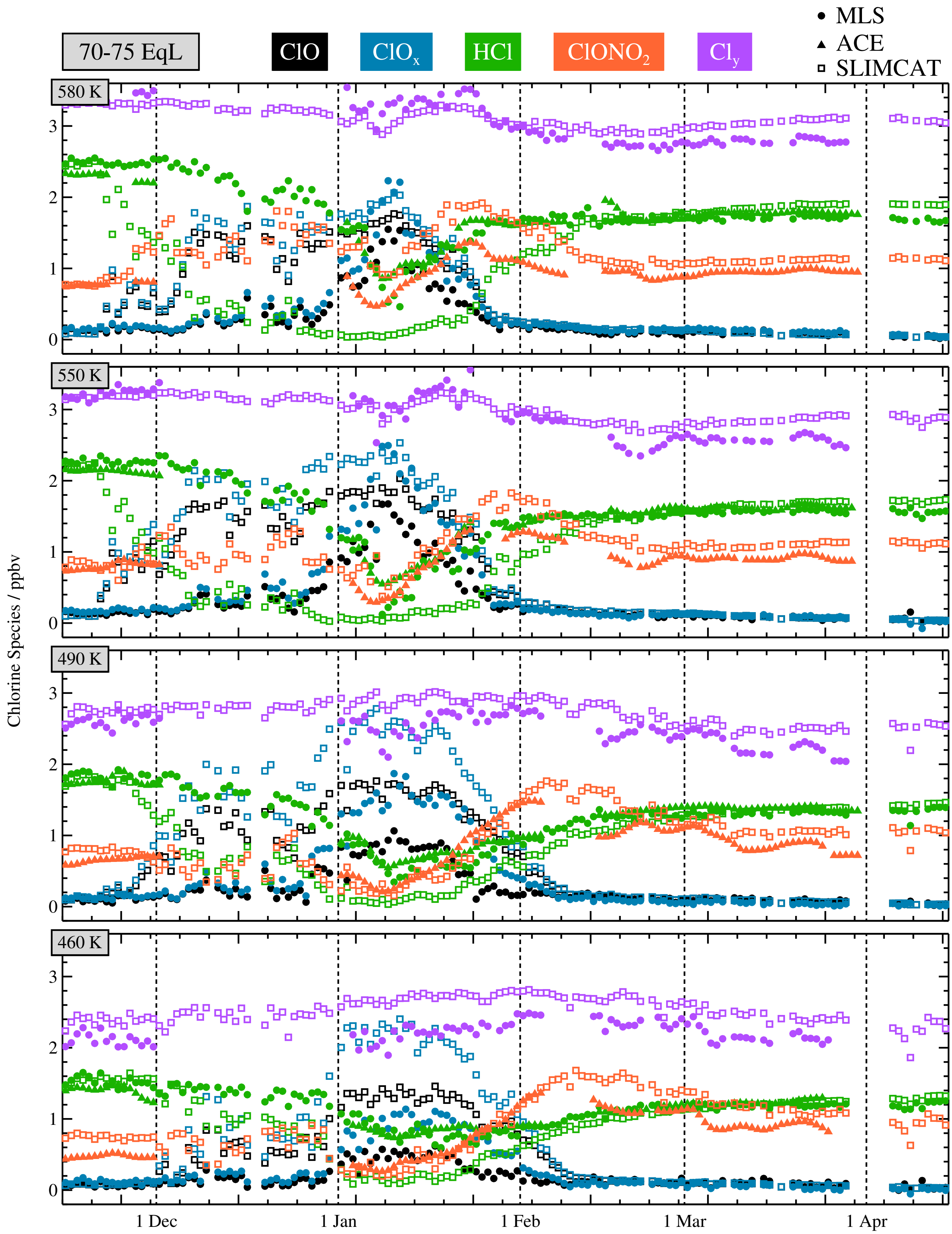

Figure 9. As in Figure 7, but for a single EqL band (70–75°EqL) at 460, 490, 550, and 580 K. (Note that this EqL band appears in Figure 7 for 520 K.)

the lower stratosphere during a brief interval in mid-August, but this is largely a sampling artifact that arises as ACE-FTS coverage of the southern high-latitude region switches from sunrise to sunset occultations, causing an interlude in which no observations are made deep in the vortex, as shown in Figure 11, skewing the vortex averages toward values more representative of the collar region than the vortex interior.

The disparity between modeled and measured quantities is less severe than in the Arctic. From late June through mid-July, measured ClO actually exceeds that from the model in much of the lower stratosphere (Figure 10). The better agreement suggests that the model's equilibrium NAT PSC scheme is more appropriate in the Antarctic, where the region of low temperatures is typically both larger and more concentric with the vortex than in the Arctic. Nevertheless, SLIMCAT again indicates earlier, more extensive, and more abrupt chemical processing. Consistent with these results, Figure 12 shows the much larger extent and degree of modeled HNO_3 depletion. Figure 12 also shows that the model calculates considerably stronger diabatic descent than indicated by MLS N_2O measurements. The vigorous descent may partially compensate for the greater chlorine activation, since modeled ozone abundances at the end of the winter are only slightly lower than those measured by MLS.

As in the Arctic, HCl greatly exceeds $ClONO_2$ (HCl/Cl_y $\sim$0.7–0.8, $ClONO_2/Cl_y$ $\sim$0.2–0.3) at southern midlatitudes (not shown) and at high latitudes before significant processing. Figure 13 shows the high-EqL averages at 520 K, near the altitude of maximum activation. Many fewer points appear at the highest EqLs than in the corresponding plots for the Arctic, where more distortion of the vortex leads to greater data coverage in sunlit conditions in early winter. HCl drops rapidly and by late June/early July approaches zero poleward of 60° EqL. $ClONO_2$ also approaches zero at the highest EqLs but does not drop below $\sim$0.2–0.4 ppbv at 65–70° EqL, and it increases over initial values at 60–65° EqL as the $ClONO_2$ collar develops. Chlorine becomes fully activated ($ClO_x/Cl_y \sim$ 0.9–1.0) at the highest EqLs by early July and remains so until early September, when deactivation commences.

At first glance, the EqL-band averages in Figure 13 appear to indicate that $ClONO_2$ and HCl recover at roughly the same rates at the end of winter, contrary to previous studies, which have found preferential reformation of HCl in Antarctic spring [e.g., *Douglass et al.*, 1995; *Santee et al.*, 1996; *Grooß et al.*, 1997; *Mickley et al.*, 1997; *Michelsen et al.*, 1999]. Unlike in the Arctic, however, ACE-FTS and MLS HCl measurements are not in good agreement in late winter even at the highest EqLs (compare Figure 13 with Figures 3 and 7), suggesting that they are sampling different air masses. This is confirmed in Figure 14, which shows oscillations or sharp changes in ACE-FTS N_2O, CH_4, O_3, and HNO_3 in all EqL bands in September. This pattern is characteristic of abrupt changes in the region of the vortex sampled by ACE-FTS, consistent with the shift in the sunset occultations from the highest latitudes deep inside the vortex to near or just outside the vortex edge during this period, as illustrated in Figure 15. This transit through the collar region imposes increases in ACE-FTS HCl and $ClONO_2$ on top of those caused by chemistry, complicating interpretation of the chlorine partitioning.

By the end of the study period, MLS registers HCl abundances of 2.5–3.0 ppbv throughout most of the vortex (Figure 13), considerably higher than those observed before the onset of chemical processing. In fact, the HCl measured in mid-October is roughly comparable to the pre-winter estimate of Cl_y, implying that $ClONO_2$ values are extremely low at this time. Few season-long HCl data records exist to compare this result against, but it is consistent with previous studies based on measurements from the Michelson Interferometer for Passive Atmospheric Sounding (MIPAS) [*Höpfner et al.*, 2004] and the UARS Cryogenic Limb Array Etalon Spectrometer (CLAES) [*Roche et al.*, 1994], which found $ClONO_2$ mixing ratios in Antarctic spring (October/November) to be lower than those at the start of winter.

Although measured and modeled chlorine species generally match much better than in the Arctic, during the deactivation phase agreement between SLIMCAT and MLS HCl varies with EqL. Despite slightly overestimating activation in September at the highest EqLs, SLIMCAT overestimates HCl as measured by MLS. At 65–70° EqL, SLIMCAT and MLS HCl agree well throughout September. Near the vortex edge, SLIMCAT significantly underestimates HCl. Even where SLIMCAT matches MLS HCl in September, however, it underestimates it by mid-October, because the model partitions a nonnegligible amount of chlorine into $ClONO_2$, such that $ClONO_2$ approximately equals that calculated in the fall. A fundamentally similar picture of chlorine activation and deactivation is seen throughout the lower stratosphere, although slight differences in the magnitude or duration of the model/measurement discrepancy are found (not shown).

4.2. The 2004 Late Antarctic Winter

Lower stratospheric minimum temperatures were below average and the vortex was unusually strong during the first half of the 2004 Antarctic winter. After MLS began routine science operations in mid-August, however, lower stratospheric temperatures rose and remained near average [*Santee et al.*, 2005]. Conditions near the top of the ozone hole ($\sim$580–550 K) were even warmer, with vortex minimum temperatures significantly higher than in other recent years

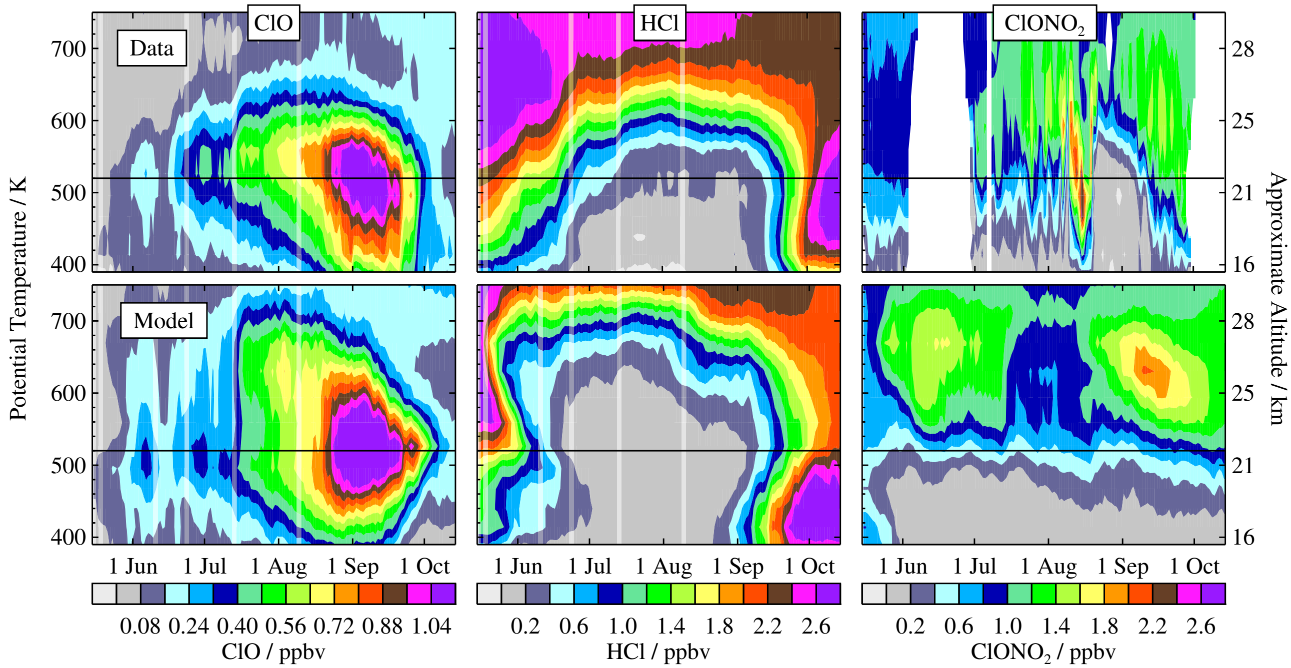

Figure 10. As in Figure 1, averaged within the $1.4\times10^{-4}\,s^{-1}$ sPV contour for the 2005 Antarctic winter. The black horizontal line in each panel marks the 520 K level.

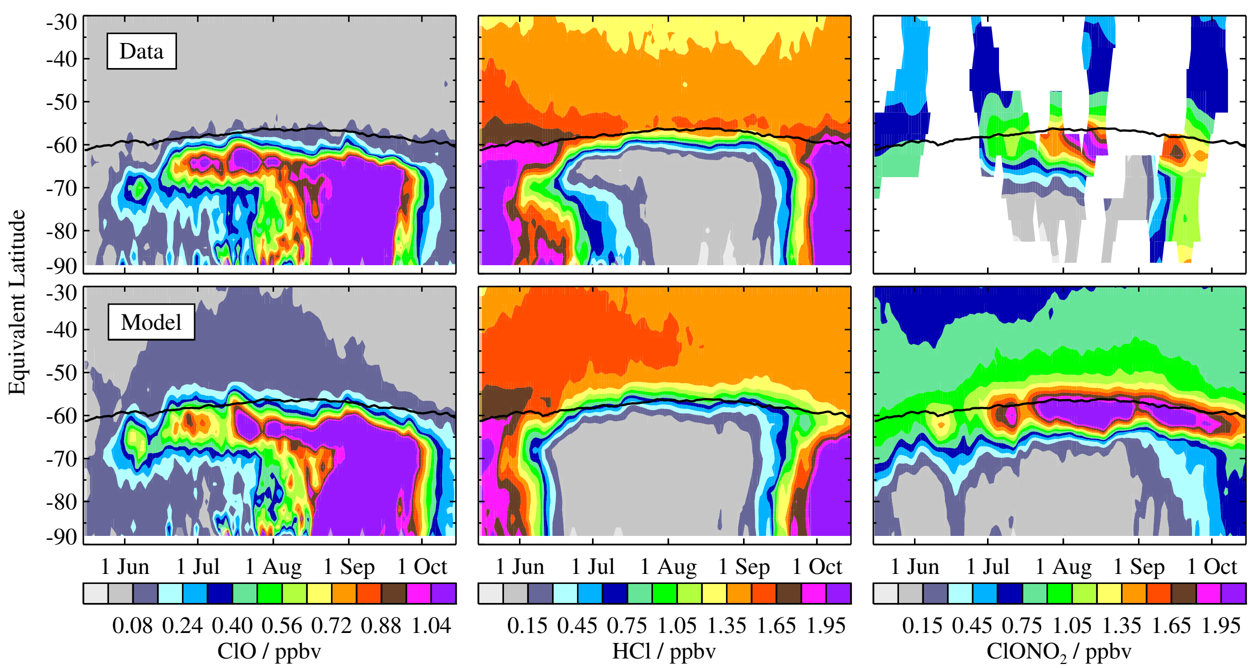

Figure 11. As in Figure 2, for the 2005 Antarctic winter at 520 K. The $1.4\times10^{-4}\,s^{-1}$ contour of sPV is overlaid in black to demark the approximate edge of the polar vortex.

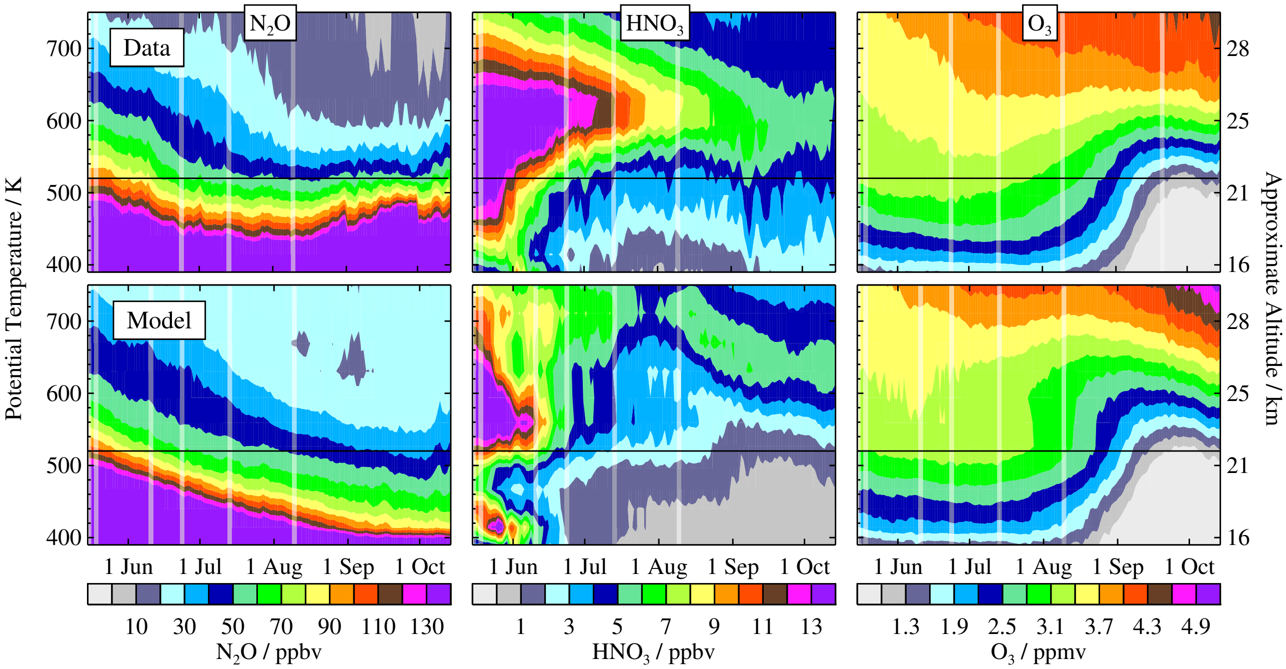

Figure 12. As in Figure 5, averaged within the 1.4×10^{-4} s^{-1} sPV contour for the 2005 Antarctic winter. The black horizontal line in each panel marks the 520 K level.

throughout most of August and September [*Hoppel et al.*, 2005]. Dynamical activity was also stronger than typical [*World Meteorological Organization*, 2007].

Comparison of Figures 13 and 16 indicates that the warmer and more dynamically disturbed conditions in the latter half of the 2004 winter led to considerably less extensive processing and an earlier retreat from maximum chlorine activation than in 2005, consistent with the much smaller degree of ozone loss than in most other recent winters, including 2005 [*Hoppel et al.*, 2005; *World Meteorological Organization*, 2007]. Nevertheless, chlorine deactivation proceeds in a very similar manner in the two winters, with MLS indicating a rapid rise in HCl in September. HCl abundances in mid-October, however, are slightly lower than those in 2005, especially at lower EqLs. $ClONO_2$ behavior is very similar to that observed in 2005, again apparently implying that the two reservoirs recover at comparable rates. Because the ACE-FTS coverage pattern repeats from year to year, the same issues discussed in section 4.1 arise in disentangling chemical, dynamical, and sampling effects and determining the relative recovery rates of the chlorine reservoirs based on the ACE-FTS data.

As in other winters studied here, SLIMCAT overestimates chlorine activation. The mismatch between modeled and measured HCl in late September and October is larger at high EqLs but smaller near the vortex edge than in 2005. In most bins the curves have converged by the end of the period, with modeled and measured HCl in fairly good agreement.

5. Summary and Conclusions

We use a suite of Aura MLS and ACE-FTS measurements from two Arctic and two Antarctic winters to investigate interannual and interhemispheric variability in chlorine partitioning throughout the lower stratosphere (400–750 K). Theoretical understanding of chlorine activation and deactivation is assessed by comparing the measurements to customized runs of the recently-updated SLIMCAT 3D chemical transport model.

In both hemispheres at middle latitudes, and at high latitudes before the onset of chlorine activation, HCl greatly exceeds $ClONO_2$, representing ∼0.7–0.8 of Cl_y (estimated from MLS ClO and HCl and ACE-FTS $ClONO_2$), compared to ∼0.2–0.3 for $ClONO_2$. Measured and modeled values typically agree well at these locations/times.

The 2004/2005 Arctic winter is the coldest on record in the lower stratosphere, causing extensive heterogeneous chemical processing. MLS observes ClO enhancement at the highest equivalent latitudes starting in early to middle December. Although HCl declines throughout the activation period, it continues to exceed $ClONO_2$ until late January, at which time each reservoir represents only ∼0.1 of

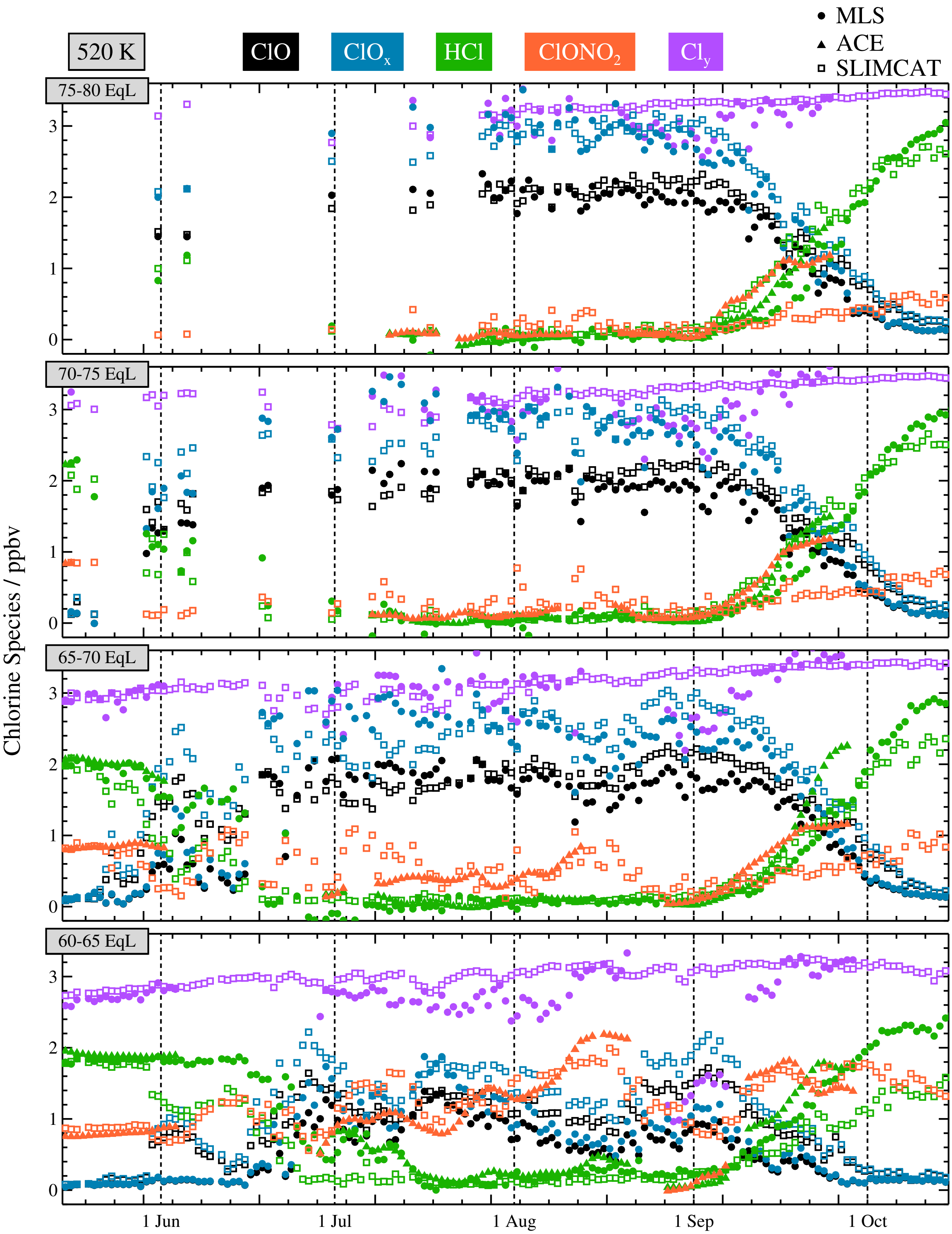

Figure 13. As in Figure 3, for the 2005 Antarctic winter at 520 K.

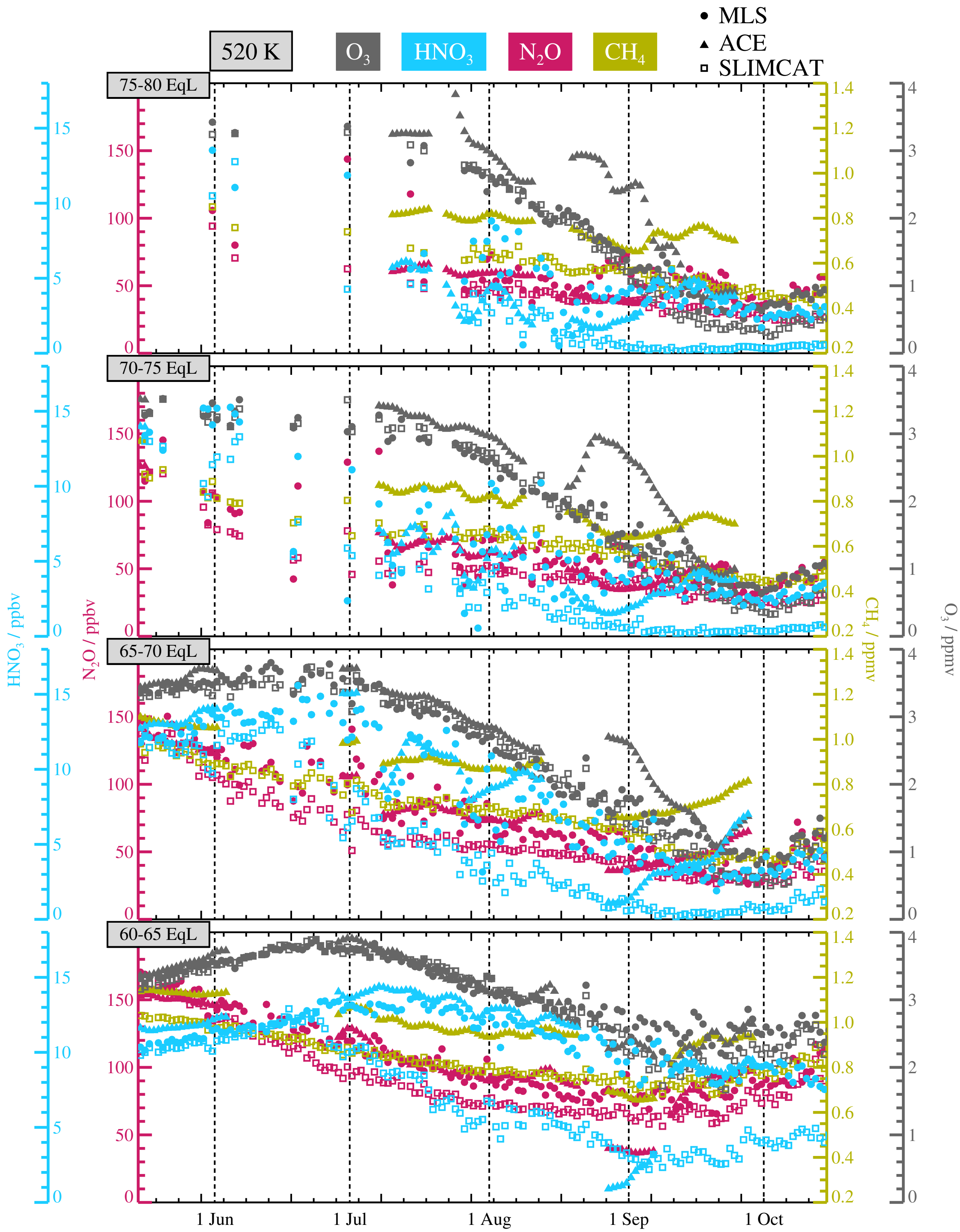

Figure 14. As in Figure 8, for the 2005 Antarctic winter at 520 K.

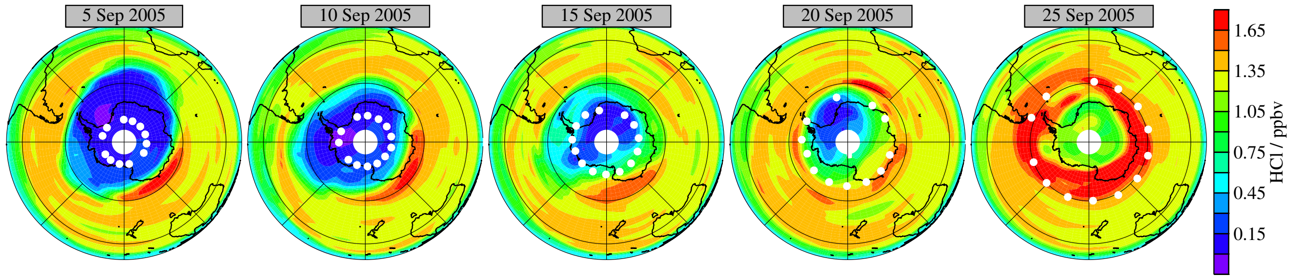

Figure 15. Maps of MLS HCl for selected days in September 2005, interpolated to 520 K. Overlaid white dots indicate the ACE-FTS occultation locations.

Cl_y in the vortex core, with ClO_x/Cl_y reaching ∼0.8–0.9. ClO then begins to decrease in early to middle February as lower stratospheric temperatures rise. ACE-FTS $ClONO_2$ increases throughout the vortex beginning in early February, whereas HCl from both ACE-FTS and MLS remains low and relatively constant until late February or early March. $ClONO_2$ peaks in early-to-middle March, at mixing ratios much higher than observed at the beginning of winter. $ClONO_2$ then slowly declines as chlorine is shifted into HCl, which has not quite recovered to pre-winter abundances by the end of the study period (15 April), when HCl/Cl_y and $ClONO_2/Cl_y$ are roughly comparable (∼0.4–0.6). A fundamentally similar picture is seen throughout the lower stratosphere. Thus MLS and ACE-FTS provide consistent evidence that chlorine deactivation in the 2004/2005 Arctic winter occurred through the initial reformation of $ClONO_2$ followed by the slow repartitioning between $ClONO_2$ and HCl, in agreement with the canonical view of Arctic chlorine recovery.

A different picture of chlorine recovery emerges from the 2005/2006 Arctic winter. Initially a strong cold vortex leads to substantial chlorine activation several weeks earlier than in 2004/2005, but a major warming in mid-January curtails chemical processing. Deactivation proceeds with HCl rising at roughly the same rate as $ClONO_2$ near the vortex edge. $ClONO_2$ reforms first and briefly surpasses HCl in the vortex core, but even there it plays a less important role than in 2004/2005. Detailed examination shows that where January 2006 ozone mixing ratios are similar to those in 2005, $ClONO_2$ recovery precedes that of HCl, whereas where they are ∼0.5 ppmv less, $ClONO_2$ and HCl recovery rates are comparable. This appears to be consistent with the results of *Douglass and Kawa* [1999], who found that low ozone and low temperatures combined to push chlorine partitioning toward HCl in spring 1997.

The Southern Hemisphere winters studied here also cover both cold (2005) and relatively warm and disturbed (2004) conditions. Unlike in the north, however, the meteorological situations are sufficiently similar that chlorine deactivation proceeds in the same manner. ClO, which is enhanced in the sunlit portions of the vortex by late May, starts to decline in late August or early September, at which time MLS observes a rapid rise in HCl. ACE-FTS suggests that $ClONO_2$ recovers at roughly the same rate as HCl, contrary to results from previous studies. ACE-FTS measurements of HCl (and other species) do not agree well with those from MLS, however, indicating that the instruments sample different air masses. These sampling differences preclude definitive interpretation of changes in chlorine partitioning. By mid-October, MLS HCl is considerably higher throughout the vortex than measured at the beginning of winter, implying extremely low values of $ClONO_2$. An essentially similar pattern of chlorine activation and deactivation is observed throughout the lower stratosphere.

Although modeled and measured values generally agree well outside the winter polar regions, SLIMCAT overestimates the magnitude, spatial extent, and duration of chlorine activation inside the polar vortices. The most likely cause of this discrepancy is SLIMCAT's PSC parameterization. Because the standard model employs an equilibrium scheme that calculates NAT PSC particles to be present whenever they are thermodynamically allowed, modeled chlorine activation begins earlier and lasts longer than indicated by the measurements, particularly in the Arctic. Chlorine deactivation follows a path similar to that seen in the data, but the longevity of modeled PSC activity induces a shift of several weeks in its timing. In general, the disparity between modeled and measured quantities is smaller in the Antarctic, where the equilibrium PSC scheme is perhaps more suitable than in the Arctic. Our results highlight the need for more accurate modeling of PSC processes, such as the 3D Lagrangian NAT particle sedimentation model used with SLIMCAT in studies of Arctic denitrification by *Davies et al.* [2005, 2006]. Incorporation of a microphysical model into the full-chemistry version of SLIMCAT is required to fully exploit the wealth of observations available for refining our understanding of polar chlorine partitioning.

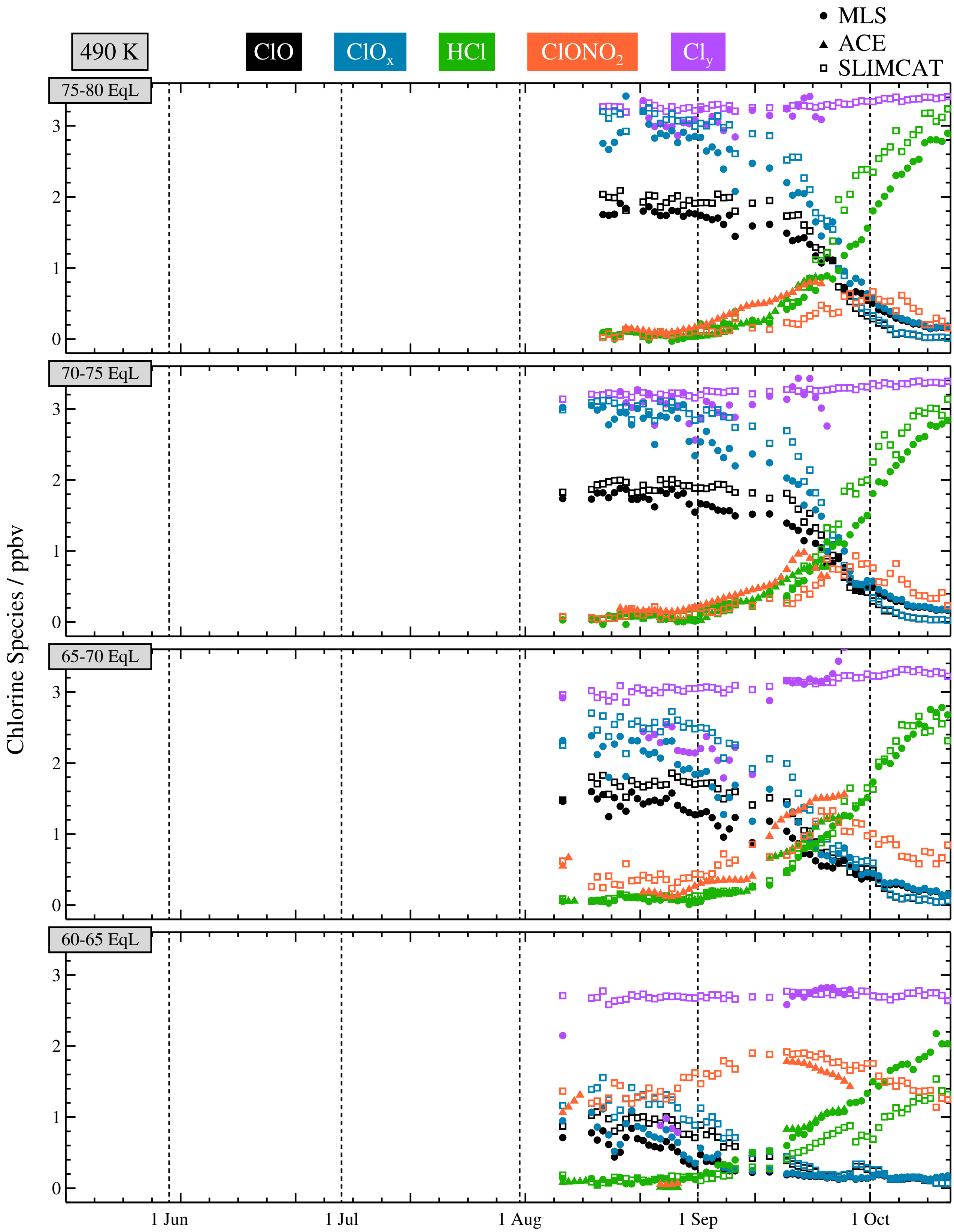

Figure 16. As in Figure 3, for the 2004 Antarctic winter.

Acknowledgments. William Daffer, Brian Knosp, and Mark Filipiak are thanked for programming support, data management, and assistance with the MLS, ACE-FTS, and SLIMCAT files. Helpful discussions with Anne Douglass and Doug Kinnison are gratefully acknowledged. Funding for ACE was provided by the Canadian Space Agency and the Natural Sciences and Engineering Research Council (NSERC) of Canada. Work at the Jet Propulsion Laboratory, California Institute of Technology, was done under contract with the National Aeronautics and Space Administration.

References

Adrian, G. P., et al., First results of ground–based FTIR measurements of atmospheric trace gases in North Sweden and Greenland during EASOE, *Geophys. Res. Lett.*, *21*, 1343–1346, 1994.

Barret, B., et al., Intercomparisons of trace gas profiles from the Odin/SMR and Aura/MLS limb sounders, *J. Geophys. Res.*, *111*, D21302, doi:10.1029/2006JD007305, 2006.

Bernath, P. F., et al., Atmospheric Chemistry Experiment (ACE): Mission overview, *Geophys. Res. Lett.*, *32*, L15S01, doi:10.1029/2005GL022386, 2005.

Blom, C. E., H. Fischer, N. Glatthor, T. Gulde, M. Höpfner, and C. Piesch, Spatial and temporal variability of $ClONO_2$, HNO_3, and O_3 in the Arctic winter of 1992/1993 as obtained by airborne infrared emission spectroscopy, *J. Geophys. Res.*, *100*, 9101–9114, 1995.

Bloom, S. C., et al., The Goddard Earth Observing Data Assimilation System, GEOS DAS Version 4.0.3: Documentation and validation, *Tech. Rep. 104606 V26*, NASA, 2005.

Blumenstock, T., H. Fischer, A. Friedle, F. Hase, and P. Thomas, Column amounts of $ClONO_2$, HCl, HNO_3, and HF from ground-based FTIR measurements made near Kiruna, Sweden, in late winter 1994, *J. Atmos. Chem.*, *26*, 311–321, 1997.

Boone, C. D., R. Nassar, K. A. Walker, Y. Rochon, S. D. McLeod, C. P. Rinsland, and P. F. Bernath, Retrievals for the atmospheric chemistry experiment Fourier-transform spectrometer, *Appl. Opt.*, *44*, 7218–7231, 2005.

Burkholder, J. B., J. J. Orlando, and C. J. Howard, Ultraviolet-absorption cross-sections of Cl_2O_2 between 210 and 410 nm, *J. Phys. Chem.*, *94*, 687–695, 1990.

Butchart, N., and E. E. Remsberg, The area of the stratospheric polar vortex as a diagnostic for tracer transport on an isentropic surface, *J. Atmos. Sci.*, *43*, 1319–1339, 1986.

Chipperfield, M. P., Multiannual simulations with a three-dimensional chemical transport model, *J. Geophys. Res.*, *104*, 1781–1805, 1999.

Chipperfield, M. P., New version of the TOMCAT/SLIMCAT off-line chemical transport model: Intercomparison of stratospheric tracer experiments, *Q. J. Roy. Meteor. Soc.*, *132*, 1179–1203, 2006.

Chipperfield, M. P., A. M. Lee, and J. A. Pyle, Model calculations of ozone depletion in the Arctic polar vortex for 1991/92 to 1994/95, *Geophys. Res. Lett.*, *23*, 559–562, 1996.

Chipperfield, M. P., E. R. Lutman, J. A. Kettleborough, J. A. Pyle, and A. E. Roche, Model studies of chlorine deactivation and formation of $ClONO_2$ collar in the Arctic polar vortex, *J. Geophys. Res.*, *102*, 1467–1478, 1997.

Chipperfield, M. P., W. Feng, and M. Rex, Arctic ozone loss and climate sensitivity: Updated three-dimensional model study, *Geophys. Res. Lett.*, *32*, L11813, doi:10.1029/2005GL022674, 2005.

Davies, S., G. W. Mann, K. S. Carslaw, M. P. Chipperfield, J. J. Remedios, G. Allen, A. M. Waterfall, R. Spang, and G. C. Toon, Testing our understanding of Arctic denitrification using MIPAS-E satellite measurements in winter 2002/2003, *Atmos. Chem. Phys.*, *6*, 3149–3161, 2006.

Davies, S., et al., Modeling the effect of denitrification on Arctic ozone depletion during winter 1999/2000, *J. Geophys. Res.*, *107*, 8322, doi:10.1029/2001JD000445, 2002.

Davies, S., et al., 3D microphysical model studies of Arctic denitrification: Comparison with observations, *Atmos. Chem. Phys.*, *5*, 3093–3109, 2005.

de Zafra, R. L., J. M. Reeves, and D. T. Shindell, Chlorine monoxide in the Antarctic spring vortex, 1. Evolution of midday vertical profiles over McMurdo Station, 1993, *J. Geophys. Res.*, *100*, 13,999–14,007, 1995.

Douglass, A., and S. Kawa, Contrast between 1992 and 1997 high-latitude spring Halogen Occultation Experiment observations of lower stratospheric HCl, *J. Geophys. Res.*, *104*, 18,739–18,754, 1999.

Douglass, A. R., M. R. Schoeberl, R. S. Stolarski, J. W. Waters, J. M. Russell, A. E. Roche, and S. T. Massie, Interhemispheric differences in springtime production of HCl and $ClONO_2$ in the polar vortices, *J. Geophys. Res.*, *100*, 13,967–13,978, 1995.

Dufour, G., et al., Partitioning between the inorganic chlorine reservoirs HCl and $ClONO_2$ during the Arctic winter 2005 from the ACE-FTS, *Atmos. Chem. Phys.*, *6*, 2355–2366, 2006.

Feng, W., M. P. Chipperfield, S. Davies, P. von der Gathen, E. Kyrö, C. M. Volk, A. Ulanovsky, and G. Belyaev, Large chemical ozone loss in 2004/2005 Arctic winter/spring, *Geophys. Res. Lett.*, *34*, L09803, doi:10.1029/2006GL029098, 2007.

Feng, W., et al., Three-dimensional model study of the Arctic ozone loss in 2002/2003 and comparison with 1999/2000 and 2003/2004, *Atmos. Chem. Phys.*, *5*, 139–152, 2005.

Froidevaux, L., et al., Early validation analyses of atmospheric profiles from EOS MLS on the Aura satellite, *IEEE Trans. Geosci. Remote Sensing*, *44*, 1106–1121, 2006.

Froidevaux, L., et al., Validation of Aura Microwave Limb Sounder HCl measurements, *J. Geophys. Res.*, *submitted*, doi:10.1029/2007JD009025, 2007, available at http://mls.jpl.nasa.gov.

Galle, B., J. Mellqvist, D. Arlander, I. Fløisand, M. Chipperfield, and A. Lee, Ground based FTIR measurements of stratospheric species from Harestua, Norway during SESAME and comparison with models, *J. Atmos. Chem.*, *32*, 147–164, 1999.

Gobiet, A., U. Foelsche, A. K. Steiner, M. Borsche, G. Kirchengast, and J. Wicker, Climatological validation of stratospheric temperatures in ECMWF operational analyses with CHAMP radio occultation data, *Geophys. Res. Lett.*, *32*, L12806, doi:10.1029/2005GL022617, 2005.

Goutail, F., et al., Early unusual ozone loss during the Arctic winter 2002/2003 compared to other winters, *Atmos. Chem. Phys.*, *5*, 665–677, 2005.

Grooß, J.-U., R. B. Pierce, P. J. Crutzen, W. L. Grose, and J. M. Russell, Re-formation of chlorine reservoirs in southern hemisphere polar spring, *J. Geophys. Res.*, *102*, 13,141–13,152, 1997.

Grooß, J.-U., G. Günther, R. Müller, P. Konopka, S. Bausch, H. Schlager, C. Voigt, C. M. Volk, and G. C. Toon, Simulation of denitrification and ozone loss for the Arctic winter 2002/2003, *Atmos. Chem. Phys.*, *5*, 1437–1448, 2005.

Hanson, D., and K. Mauersberger, Laboratory studies of the nitric acid trihydrate: Implications for the south polar stratosphere, *Geophys. Res. Lett.*, *15*, 855–858, 1988.

Hanson, D. R., and A. R. Ravishankara, Reactive uptake of $ClONO_2$ onto sulfuric acid due to reaction with HCl and H_2O, *J. Phys. Chem.*, *98*, 5728–5735, 1994.

Höpfner, M., et al., First spaceborne observations of Antarctic stratospheric $ClONO_2$ recovery: Austral spring 2002, *J. Geophys. Res.*, *109*, D11308, doi:10.1029/2004JD004609, 2004.

Höpfner, M., et al., Validation of MIPAS $ClONO_2$ measurements, *Atmos. Chem. Phys.*, *7*, 257–281, 2007.

Hoppel, K., G. Nedoluha, M. Fromm, D. Allen, R. Bevilacqua, J. Alfred, B. Johnson, and G. König-Langlo, Reduced ozone loss at the upper edge of the Antarctic Ozone Hole during 2001–2004, *Geophys. Res. Lett.*, *32*, L20816, doi:10.1029/2005GL023968, 2005.

Jin, J. J., et al., Severe arctic ozone loss in the winter 2004/2005: Observations from ACE-FTS, *Geophys. Res. Lett.*, *33*, L15801, doi:10.1029/2006GL026752, 2006.

Kleinböhl, A., et al., Denitrification in the Arctic mid-winter 2004/2005 observed by airborne submillimeter radiometry, *Geophys. Res. Lett.*, *32*, L19811, doi:10.1029/2005GL023408, 2005.

Kreher, K., J. G. Keys, P. V. Johnston, U. Platt, and X. Liu, Ground-based measurements of OClO and HCl in austral spring 1993 at Arrival Heights, Antarctica, *Geophys. Res. Lett.*, *23*, 1545–1548, 1996.

Liu, X., R. D. Blatherwick, F. J. Murcray, J. G. Keys, and S. Solomon, Measurements and model calculations of HCl column amounts and related parameters over McMurdo during the austral spring in 1989, *J. Geophys. Res.*, *97*, 20,795–20,804, 1992.

Livesey, N. J., W. V. Snyder, W. G. Read, and P. A. Wagner, Retrieval algorithms for the EOS Microwave Limb Sounder (MLS), *IEEE Trans. Geosci. Remote Sensing*, *44*, 1144–1155, 2006.

Livesey, N. J., et al., Version 1.5 Level 2 data quality and description document, *Tech. Rep. JPL D-32381*, Jet Propulsion Laboratory, 2005, available from http://mls.jpl.nasa.gov.

Luo, B., K. S. Carslaw, T. Peter, and S. L. Clegg, Vapour pressures of $H_2SO_4/HNO_3/HCl/HBr/H_2O$ solutions to low stratospheric temperatures, *Geophys. Res. Lett.*, *22*, 247–250, 1995.

Lutman, E. R., R. Toumi, R. L. Jones, D. J. Lary, and J. A. Pyle, Box model studies of ClO_x deactivation and ozone loss during the 1991/92 northern hemisphere winter, *Geophys. Res. Lett.*, *21*, 1415–1418, 1994.

MacKenzie, I. A., R. S. Harwood, L. Froidevaux, W. G. Read, and J. W. Waters, Chemical loss of polar vortex ozone inferred from UARS MLS measurements of ClO during the Arctic and Antarctic late winters of 1993, *J. Geophys. Res.*, *101*, 14,505–14,518, 1996.

Mann, G. W., S. Davies, K. S. Carslaw, M. P. Chipperfield, and J. Kettleborough, Polar vortex concentricity as a controlling factor in Arctic denitrification, *J. Geophys. Res.*, *107*, 4663, doi:10.1029/2002JD002102, 2002.

Mann, G. W., S. Davies, K. S. Carslaw, and M. P. Chipperfield, Factors controlling Arctic denitrification in cold winters of the 1990s, *Atmos. Chem. Phys.*, *3*, 403–416, 2003.

Mann, G. W., K. S. Carslaw, M. P. Chipperfield, S. Davies, and S. D. Eckermann, Large nitric acid trihydrate particles and denitrification caused by mountain waves in the Arctic stratosphere, *J. Geophys. Res.*, *110*, D08202, doi:10.1029/2004JD005271, 2005.

Manney, G. L., M. L. Santee, L. Froidevaux, K. Hoppel, N. J. Livesey, and J. W. Waters, EOS MLS observations of ozone loss in the 2004–2005 Arctic winter, *Geophys. Res. Lett.*, *33*, L04802, doi:10.1029/2005GL024494, 2006.

Manney, G. L., et al., On the motion of air through the stratospheric polar vortex, *J. Atmos. Sci.*, *51*, 2973–2994, 1994.

Manney, G. L., et al., Solar occultation satellite data and derived meteorological products: Sampling issues and comparisons with Aura MLS, *J. Geophys. Res.*, *submitted*, doi:10.1029/2007JD008709, 2007, available at http://mls.jpl.nasa.gov.

Mellqvist, J., et al., Ground-based FTIR observations of chlorine activation and ozone depletion inside the Arctic vortex during the winter of 1999/2000, *J. Geophys. Res.*, *107*, 10.1029/2001JD001080, 2002.

Michelsen, H. A., et al., Maintenance of high HCl/Cl_y and NO_x/NO_y in the Antarctic vortex: A chemical signature of confinement during spring, *J. Geophys. Res.*, *104*, 26,419–26,436, 1999.

Mickley, L. J., J. P. D. Abbatt, J. E. Frederick, and J. M. Russell, Evolution of chlorine and nitrogen species in the lower stratosphere during Antarctic spring: Use of tracers to determine chemical change, *J. Geophys. Res.*, *102*, 21,479–21,491, 1997.

Müller, R., T. Peter, P. J. Crutzen, H. Oelhaf, G. P. Adrian, T. von Clarmann, A. Wegner, U. Schmidt, and D. Lary, Chlorine chemistry and the potential for ozone depletion in the Arctic stratosphere in the winter of 1991/92, *Geophys. Res. Lett.*, *21*, 1427–1430, 1994.

Müller, R., P. J. Crutzen, J.-U. Grooß, C. Brühl, J. M. Russell, and A. F. Tuck, Chlorine activation and ozone depletion in the Arctic vortex: Observations by the Halogen Occultation Experiment on the Upper Atmosphere Research Satellite, *J. Geophys. Res.*, *101*, 12,531–12,554, 1996.

Murcray, F. J., A. Goldman, R. Blatherwick, A. Matthews, and N. Jones, HNO_3 and HCl amounts over McMurdo during the spring of 1987, *J. Geophys. Res.*, *94*, 16,615–16,618, 1989.

Notholt, J., G. Toon, R. Lehmann, B. Sen, and J.-F. Blavier, Comparison of Arctic and Antarctic trace gas column abundances from ground-based Fourier transform infrared spectrometry, *J. Geophys. Res.*, *102*, 12,863–12,869, 1997a.

Notholt, J., G. Toon, F. Stordal, S. Solberg, N. Schmidbauer, E. Becker, A. Meier, and B. Sen, Seasonal variations of atmospheric trace gases in the high Arctic at 79°N, *J. Geophys. Res.*, *102*, 12,855–12,861, 1997b.

Oelhaf, H., T. von Clarmann, H. Fischer, F. Friedl-Vallon, C. Fritzsche, A. Linden, C. Piesch, M. Seefeldner, and W. Völker, Stratospheric $ClONO_2$ and HNO_3 profiles inside the Arctic vortex from MIPAS-B limb emission spectra obtained during EASOE, *Geophys. Res. Lett.*, *21*, 1263–1266, 1994.

Payan, S., C. Camry-Peyret, P. Jeseck, T. Hawat, G. Durry, and F. Lefèvre, First direct simultaneous HCl and $ClONO_2$ profile measurements in the Arctic vortex, *Geophys. Res. Lett.*, *25*, 2663–2666, 1998.

Prather, M., and A. H. Jaffe, Global impact of the Antarctic ozone hole: Chemical propagation, *J. Geophys. Res.*, *95*, 3473–3492, 1990.

Rex, M., et al., Arctic winter 2005: Implications for stratospheric ozone loss and climate change, *Geophys. Res. Lett.*, *33*, L23808, doi:10.1029/2006GL026731, 2006.

Roche, A. E., et al., Observations of lower-stratospheric $ClONO_2$, HNO_3, and aerosol by the UARS CLAES experiment between January 1992 and April 1993, *J. Atmos. Sci.*, *51*, 2877–2902, 1994.

Sander, S. P., R. R. Friedl, and Y. L. Yung, Rate of formation of the ClO dimer in the polar stratosphere: Implications for ozone loss, *Science*, *245*, 1095–1098, 1989.

Sander, S. P., et al., Chemical kinetics and photochemical data for use in atmospheric studies: Evaluation number 14, *Tech. Rep. JPL Publ. 02-25*, Jet Propulsion Laboratory, 2003.

Santee, M. L., G. L. Manney, J. W. Waters, and N. J. Livesey, Variations and climatology of ClO in the polar lower stratosphere from UARS Microwave Limb Sounder measurements, *J. Geophys. Res.*, *108*, 4454, doi:10.1029/2002JD003335, 2003.

Santee, M. L., G. L. Manney, N. J. Livesey, and W. G. Read, Three-dimensional structure and evolution of stratospheric HNO_3 based on UARS Microwave Limb Sounder measurements, *J. Geophys. Res.*, *109*, D15306, doi:10.1029/2004JD004578, 2004.

Santee, M. L., et al., Chlorine deactivation in the lower stratospheric polar regions during late winter: Results from UARS, *J. Geophys. Res.*, *101*, 18,835–18,859, 1996.

Santee, M. L., et al., Polar processing and development of the 2004 Antarctic ozone hole: First results from MLS on Aura, *Geophys. Res. Lett.*, *32*, L12817, doi:10.1029/2005GL022582, 2005.

Santee, M. L., et al., Validation of the Aura Microwave Limb Sounder ClO measurements, *J. Geophys. Res.*, *submitted*, doi:10.1029/2007JD008762, 2007a, available at http://mls.jpl.nasa.gov.

Santee, M. L., et al., Validation of the Aura Microwave Limb Sounder HNO_3 measurements, *J. Geophys. Res.*, *submitted*, doi:10.1029/2007JD008721, 2007b, available at http://mls.jpl.nasa.gov.

Schoeberl, M. R., et al., Chemical observations of a polar vortex intrusion, *J. Geophys. Res.*, *111*, D20306, doi:10.1029/2006JD007134, 2006.

Simmons, A., M. Hortal, G. Kelly, A. McNally, A. Untch, and S. Uppala, ECMWF analyses and forecasts of stratospheric winter polar vortex breakup: September 2002 in the Southern Hemisphere and related events, *J. Atmos. Sci.*, *62*, 668–689, 2005.

Singleton, C. S., et al., 2002/2003 Arctic ozone loss deduced from POAM III satellite observations and the SLIMCAT chemical transport model, *Atmos. Chem. Phys.*, *5*, 597–609, 2005.

Singleton, C. S., et al., Quantifying ozone loss during the 2004/2005 Arctic winter, *J. Geophys. Res.*, *112*, D07304, doi:10.1029/2006JD007463, 2007.

Solomon, P., B. Connor, J. Barrett, T. Mooney, A. Lee, and A. Parrish, Measurements of stratospheric ClO over Antarctica in 1996–2000 and implications for ClO dimer chemistry, *Geophys. Res. Lett.*, *29*, 10.1029/2002GL015232, 2002.

Stimpfle, R. M., D. M. Wilmouth, R. J. Salawitch, and J. G. Anderson, First measurements of ClOOCl in the stratosphere: The coupling of ClOOCl and ClO in the Arctic polar vortex, *J. Geophys. Res.*, *109*, D03301, doi:10.1029/2003JD003811, 2004.

Swinbank, R., N. B. Ingleby, P. M. Boorman, and R. J. Renshaw, A 3D variational data assimilation system for the stratosphere and troposphere, *Tech. Rep. 71*, Met Office Numerical Weather Prediction Forecasting Research Scientific Paper, 2002.

Toohey, D. W., L. M. Avallone, L. R. Lait, P. A. Newman, M. R. Schoeberl, D. W. Fahey, E. L. Woodbridge, and J. G. Anderson, The seasonal evolution of reactive chlorine in the northern hemisphere stratosphere, *Science*, *261*, 1134–1136, 1993.

Toon, G. C., C. B. Farmer, L. L. Lowes, P. W. Schaper, J.-F. Blavier, and R. H. Norton, Infrared aircraft measurements of stratospheric composition over Antarctica during September 1987, *J. Geophys. Res.*, *94*, 16,571–16,596, 1989.

Toon, G. C., J.-F. Blavier, and J. T. Szeto, Latitude variations of stratospheric trace gases, *Geophys. Res. Lett.*, *21*, 2599–2602, 1994.

von Hobe, M., et al., Severe ozone depletion in the cold Arctic winter 2004–05, *Geophys. Res. Lett.*, *33*, L17815, doi:10.1029/2006GL026945, 2006.

Waters, J. W., et al., The Earth Observing System Microwave Limb Sounder (EOS MLS) on the Aura satellite, *IEEE Trans. Geosci. Remote Sensing*, *44*, 1075–1092, 2006.

Wehr, T., S. Crewell, K. Künzi, J. Langen, H. Nett, J. Urban, and P. Hartogh, Remote sensing of ClO and HCl over northern Scandinavia in winter 1992 with an airborne submillimeter radiometer, *J. Geophys. Res.*, *100*, 20,957–20,968, 1995.

Wilmouth, D. M., R. M. Stimpfle, J. G. Anderson, J. W. Elkins, D. F. Hurst, R. J. Salawitch, and L. R. Lait, Evolution of inorganic chlorine partitioning in the Arctic polar vortex, *J. Geophys. Res.*, *111*, D16308, doi:10.1029/2005JD006951, 2006.

World Meteorological Organization, *Scientific assessment of ozone depletion: 2002*, Global Ozone Res. and Monit. Proj. Rep. No. 47, Geneva, 2003.

World Meteorological Organization, Antarctic ozone bulletin, winter/spring summary, *Tech. Rep. 8*, Global Atmosphere Watch Programme, 2005, available at http://www.wmo.int/pages/prog/arep/gaw/ozone/index.html.

World Meteorological Organization, Joint WMO/EC SCOUT-O3 Arctic ozone bulletin, winter/spring summary, *Tech. Rep. 1*, Global Atmosphere Watch Programme, 2006, available at http://www.wmo.int/pages/prog/arep/gaw/ozone/index.html.

World Meteorological Organization, *Scientific assessment of ozone depletion: 2006*, Global Ozone Res. and Monit. Proj. Rep. No. 50, Geneva, 2007.

M. L. Santee (corresponding author), L. Froidevaux, N. J. Livesey, and J. W. Waters, Jet Propulsion Laboratory, Mail Stop 183–701, 4800 Oak Grove Drive, Pasadena, CA 91109, USA. (mls@mls.jpl.nasa.gov)

I. A. MacKenzie, School of GeoSciences, The University of Edinburgh, Edinburgh EH9 3JN, UK.

G. L. Manney, Department of Physics, New Mexico Institute of Mining and Technology, Socorro, NM 87801, USA.

M. P. Chipperfield, School of the Environment, University of Leeds, Leeds, UK.

P. F. Bernath, Department of Chemistry, University of York, Heslington, York YO10 5DD, U.K.

C. D. Boone, Department of Chemistry, University of Waterloo, 200 University Ave. W., Waterloo, Ontario, Canada.

K. A. Walker, Department of Physics, University of Toronto, Toronto, Canada.

This preprint was prepared with AGU's LaTeX macros v5.01, with the extension package 'AGU^{++}' by P. W. Daly, version 1.6b from 1999/08/19.